U.S. - JAPAN COORDINATED PROGRAM

FOR

MASONRY BUILDING RESEARCH

REPORT NO. 2.2-1

FEM/I
A FINITE ELEMENT COMPUTER PROGRAM FOR THE NONLINEAR STATIC ANALYSIS OF REINFORCED MASONRY BUILDING COMPONENTS

by

ROBERT D. EWING
AHMAD M. EL–MUSTAPHA
JOHN C. KARIOTIS

DECEMBER 1987
(REVISED JUNE 1990)

supported by:

NATIONAL SCIENCE FOUNDATION

GRANT NO. CES-8696076
GRANT NO. CES-8517023

Ewing/Kariotis/Englekirk & Hart

EKEH

PREFACE

This report presents the results of a research project which was part of the U.S. Coordinated Program for Masonry Building Research. The program constitutes the United States part of the United States - Japan Coordinated Masonry Research Program conducted under the auspices of The Panel on Wind and Seismic Effects of the U.S.-Japan Natural Resources Development Program (UJNR).

The material is based on work supported by the National Science Foundation under the direction of Program Director, Dr. S.C. Liu.

PB93-213007

FEM/I

A FINITE ELEMENT COMPUTER PROGRAM FOR THE NONLINEAR STATIC ANALYSIS OF REINFORCED MASONRY BUILDING COMPONENTS

BY

ROBERT D. EWING
AHMAD M. EL-MUSTAPHA
JOHN C. KARIOTIS

DECEMBER 1987
(REVISED JUNE 1990)

SPONSORED BY

NATIONAL SCIENCE FOUNDATION
GRANT NO. CES-8696076 AND BCS-8722868
GRANT NO. CES-8517023 AND BCS-8722867

REPORT NO. 2.2-1

E K E H

EWING/KARIOTIS/ENGLEKIRK & HART
EWING & ASSOCIATES
28907 DOVERRIDGE DR.
RANCHO PALOS VERDES, CALIFORNIA 90274
(310) 541-3795

CONTENTS

CONTENTS (Continued)

LIST OF FIGURES AND TABLES

LIST OF FIGURES AND TABLES (Continued)

SECTION 1

INTRODUCTION

A coordinated, multi-year research program on reinforced masonry building components and buildings is being conducted by a team of masonry researchers organized as TCCMAR (Technical Coordinating Committee on Masonry Research) [22] under the sponsorship of the National Science Foundation (NSF). This program has several categories of research that combine experimental and analytical investigations leading to the development of experimentally validated analytical modeling techniques and design procedures.

The analytical investigations are being conducted in three integrated and coordinated tasks in the Category 2 research [8], where three basic structural engineering modeling approaches are being developed: Structural Component Models (SCMs), Finite Element Models (FEMs), and Lumped Parameter Models (LPMs). Each of the tasks provide different, but complimentary, analytical modeling approaches that are needed to effectively investigate and evaluate the nonlinear, static and dynamic response of typical reinforced masonry buildings, and to define the various limit states of the buildings and their components. The Category 2 research will lead to experimentally validated analytical models, procedures, and guidelines for the analysis of the probable response of typical reinforced masonry buildings. These methods are intended to be used by practicing structural engineers for the design and analysis of reinforced masonry buildings. Also, the analytical modeling is designed to meet the objectives of the National Earthquake Hazards Reduction Program (NEHRP) [11].

This report describes a finite element computer program or code, FEM/I, that has been developed in Task 2.2 for the nonlinear static analysis of reinforced masonry building components subjected to in-plane loading. This computer code will be used to provide element properties for the structural component models (SCMs) being developed in Task 2.1 and for the lumped parameter models (LPMs) being developed in Task 2.3. These element properties are most reliably obtained from experiments; however, it is not advisable or economically feasible to conduct a sufficient number of tests to provide data for every possible modeling

need (i.e., component size, masonry strength, vertical and horizontal reinforcement percentages, loading conditions, etc.). An analytical model that has been verified and validated with a series of complimentary tests [25] is ideally suited to provide the element properties for the SCMs and LPMs. Accordingly, one of the main purposes of this task, Task 2.2, is to develop an analytical procedure to define these element properties for the in-plane response of reinforced masonry walls, and to provide this data for configurations that will not be tested, as well as provide data that cannot be measured. These properties are a function of geometry, reinforcement, masonry materials, and loading conditions. In addition to the properties, the model will provide quantitative information on the sequence of events leading to failure and data that relates ductility to damage. These models will also provide quantitative data to aid in the interpretation of the experimental results.

The FEM/I computer program will undergo changes and improvements as the overall TCCMAR program progresses, and this report describes the current version of the code (Version 105) that was developed in the first phase of the Category 2, Task 2.2 research on strain analysis models for reinforced masonry building components. This work is being released in its current state of development so that other members of the TCCMAR research group can have access to the analytical tools as they are developed. After being validated by the experiments, the computer program will be used to analyze configurations that have not been tested, thereby extending the base of available data for the development of the SCMs and LPMs. General distribution of the final version of the computer program to the engineering profession will be accomplished through NISEE (National Information Service for Earthquake Engineering), Earthquake Engineering Research Center, University of California, Berkeley, California.

Computer Code Background - This computer program is based on the VISCOUNT family of computer programs originally developed by E. Hinton and D. R. J. Owen [23]. The VISCOUNT program was subsequently modified and improved by others [1], and the FEM/I code utilizes some of the features of the original and improved versions of the code. However, the code has been extensively modified and improved for application to reinforced masonry building components.

Report Organization - Section 2 gives a general description of the computer code. The finite element and nonlinear material models are given in Section 3, and the analytical method and computational algorithm are described in Section 4. Section 5 describes the input data required to execute the computer program. Example applications for part of the program validation are given in Section 6. Conclusions, future research work, and acknowledgements are presented in Section 7. Section 8 lists the references used in developing the computer code, mathematical models, and material models. Appendix A gives an analysis model that is intended to demonstrate the use of the FEM/I computer program and to serve as a guide for the preparation of the input data for a typical application. Some basic documentation for the computer program is provided in Appendix B. This code documentation is not intended to be complete, and is provided only as an aid to the user who may wish to modify the program. Appendix C gives differences in the definition of the input data for earlier versions of the computer program.

SECTION 2

GENERAL DESCRIPTION OF THE COMPUTER CODE

FEM/I is a nonlinear, two-dimensional finite element computer program for the static analysis of reinforced masonry building components, in-plane. This version of the FEM/I code is operational on IBM compatible personal computers, such as the 286/386/486 systems and the IBM PC/AT. This capability makes the developed technology available to a large group of interested engineers and researchers, since a large main frame computer is not required to operate the program.

Element and Material Library - The finite element library is based on a two-dimensional, parabolic isoparametric quadrilateral element and includes

- 4 node linear, quadrilateral element
- 8 node quadratic, quadrilateral element
- 9 node quadratic, quadrilateral element

This element has been thoroughly tested and has been shown to be a good performer [6, 15, and 29]. Currently, one nonlinear and one linear material model are included in the code. The nonlinear material model is designed to represent reinforced masonry or reinforced concrete under biaxial loadings and the model is described in Section 3. Although the 4, 8, and 9 node elements can be used for the linear elastic analysis, the nonlinear model for reinforced masonry uses the 4 node element.

Loading Conditions - The finite element models can be subjected to any combination of several static loading conditions including

- Nodal point forces, concentrated
- Gravity loads
- Normal and tangential distributed edge loads
- Prescribed nodal point displacements

Solution Method - The program uses an initial stiffness formulation [23 and 30] with an incremental solution method, where displacements and/or forces can be used as the primary excitation. This method is convergent for softening systems when prescribed displacements are used as the primary excitation. The code uses a frontal equation solution technique [15]. This frontal method is very efficient and has some advantages over the banded equation solution methods.

Output - The output available from the code consists of selective printed responses and a data file suitable for postprocessing by a companion program. The printed output and postprocessing data files include

- Nodal displacements
- Nodal reactions
- Stresses, both global and principal values
- Principal strains
- Reinforcing steel stresses and strains

In addition, the code produces a major event file and a force-deflection file.

Major Event File - The major event file contains a record of the major events for each element of the finite element model; namely,

- Load increment at which first tensile cracking occurs in the masonry.
- Maximum and minimum values of the tensile crack orientation in the masonry.
- Load increment at which the masonry peak strength is reached.
- Load increment at which yielding of the vertical and horizontal reinforcement occurs.
- Load increment at which the damage factor is invoked for the masonry in compression.
- Maximum strains in the vertical and horizontal reinforcement.

Force-Deflection File - The force-deflection file contains a component of the reaction force and the deflection at a node that has prescribed displacement. The reaction force can include the reactions at a series of related nodes that also have prescribed displacements. The force-deflection file is updated at each loading increment.

Sign Convention - A two-dimensional right-handed coordinate system is used to define the geometry of the finite element models (i.e., an X-Y coordinate system for plane stress or plane strain geometries and an R-Z coordinate system for axisymmetric geometries). Nodal displacements, nodal forces, and nodal reactions are positive when they are in the positive direction of the coordinate system and negative when they are in the negative direction of the coordinate system. Stresses and strains are positive when they are tensile and negative when they are compressive. The location of the Gauss points relative to the element nodal connectivity is given in Card Group 4 in Section 5 (page 49).

SECTION 3

FINITE ELEMENT MODEL

3.1 INTRODUCTION

A search of the literature and prior research findings have confirmed that the use of nonlinear finite element models is the most comprehensive analytical approach for the investigation of the limit state behavior of reinforced masonry, in-plane. A state-of-the-art review of finite element analysis of reinforced concrete structures is given in two ASCE publications; one gives the findings of an ASCE task committee [2], and the other gives the proceedings of a joint US/Japan symposium [20]. The reported research on nonlinear finite element models for reinforced concrete walls and panels demonstrates that some of the models can reasonably reproduce the degrading force-displacement envelopes up to their peak strength, as well as the relative degrees of associated damage. However, the researchers reported difficulties in reproducing the post peak strength behavior. The deficiencies that were noted by some researchers include: objectivity, difficulty in passing over the limit points, convergence, problems associated with non-positive definite stiffness matrices, and compression behavior beyond peak strength. The development of the FEM/I model was technically challenging, since it had to overcome many of the deficiencies noted by previous researchers, as well as incorporate modeling capabilities that specifically represent the behavior observed for reinforced masonry. Since prior testing has shown similarities between reinforced masonry and reinforced concrete, it is generally agreed that a technology transfer between these two materials is appropriate. Accordingly, the models developed in this research report are based on the work in reinforced concrete.

3.2 ANALYTICAL MODEL

Finite element models (FEMs) are being developed in this task to represent the static, nonlinear response of masonry components and walls, in-plane. The analytical models and constitutive relations used for reinforced masonry walls must account for the various biaxial stress states that can exist in the walls, as well as the pre- and post-cracking behavior. These walls have regions of

stress that correspond to principal stresses with tension-compression, tension-tension, and compression-compression states.

The analytical model developed in this report uses a two-dimensional finite element formulation with nonlinear stress-strain relations for the reinforced masonry. The finite element method has been widely used in the solution of nonlinear problems encountered in engineering. Problems with material nonlinearities, geometric nonlinearities, or both can be solved within an acceptable degree of accuracy. The type of nonlinearities dealt with in this report are of the material nonlinear type, and geometric nonlinearities are assumed negligible for the current version of the program. Extension of the developed models to include geometric nonlinearity is straightforward and will be adopted if found necessary during the program validation and application phases.

The masonry and reinforcement are modeled separately, and their interaction is included by using four node, isoparametric, plane stress overlay elements and specialized stress-strain relations. In the overlay or layered model, two quadrilateral elements occupy the same space, overlaying each other, where one layer represents the masonry and the other represents the reinforcement. Although the material models for the masonry and reinforcement are described separately, the element is considered to be a smeared hybrid element, where the computed strains are assigned to both materials.

The masonry is represented by a material with bimodular orthotropy, and includes tension stiffening, compression softening, and strain softening, as well as a degrading unloading rule. The material model is formulated in terms of element principal strains that correspond to the orthotropic directions. The model assumes that tension cracks are smeared over the Gauss points of the element. A crack is allowed to form when the principal tensile strain exceeds the cracking strain of the masonry, and the crack forms perpendicular to the direction of principal tensile strain. The masonry model incorporates a tension crack orientation adjustment approach, where the orientation of the final cracks can be different from the initial cracks. Experiments have shown that the final cracks do not necessarily coincide with their original orientations (i.e., a

fixed crack approach is theoretically incorrect). The model also includes a compressive strength reduction after tensile cracking normal to the principal compressive strains as shown by Vecchio and Collins [27]. The strength reduction is a function of the magnitude of the principal strains that are normal to the principal compressive strains. Additionally, the model includes a compressive strength increase due to lateral compressive confinement. The strength increase depends on the magnitude of the principal compressive stresses that are normal to the principal compressive stresses. Also, the integrity of the Gauss points is preserved in each element, where individual Gauss points can be in a different state of principal strain, thereby allowing strain gradients to occur across an element. This permits the use of relatively large elements when compared to approaches that assume average stresses and strains.

The smeared model assumes that the reinforcement is distributed over the whole element and that the two components (reinforcement and masonry) are in full bond at the nodes. The bond slip between the two components is considered to be a material property of the masonry component in tension, and this property is defined by a tension stiffening model. The reinforcement is represented by an orthotropic material with a bilinear stress-strain relationship and includes unloading.

The program uses an initial stiffness formulation with an incremental solution method, where displacements and/or forces can be used as the primary excitation. This method is a straightforward computational strategy and is reliably convergent for softening systems when prescribed displacements are used as the primary excitation. At every displacement/load increment, principal strains are calculated for each Gauss point, and secant material moduli in the principal strain directions are used to calculate the element stresses and nodal forces. The secant material matrix for the masonry uses two constitutive laws; one before tensile cracking occurs and one after tensile cracking. The constitutive law for the masonry before tensile cracking occurs is based on the Darwin and Pecknold [7] model as given below:

$$\begin{Bmatrix} \sigma_1 \\ \sigma_2 \\ \tau_{12} \end{Bmatrix} = \frac{1}{1 - \nu^2} \begin{bmatrix} E_1 & \nu(E_1E_2)^{\frac{1}{2}} & 0 \\ \nu(E_1E_2)^{\frac{1}{2}} & E_2 & 0 \\ 0 & 0 & \bar{G} \end{bmatrix} \begin{Bmatrix} \epsilon_1 \\ \epsilon_2 \\ \gamma_{12} \end{Bmatrix} \qquad (3\text{-}1)$$

where E_1 and E_2 are the secant material moduli in the two principal strain directions, ν is Poisson's ratio, and the shear modulus, $\bar{G}$, is given by

$$\bar{G} = 1/4 \left[E_1 + E_2 - 2\nu(E_1E_2)^{\frac{1}{2}} \right] \qquad (3\text{-}2)$$

After tensile cracking the constitutive law for the masonry is given by

$$\begin{Bmatrix} \sigma_1 \\ \sigma_2 \\ \tau_{12} \end{Bmatrix} = \begin{bmatrix} E_1 & 0 & 0 \\ 0 & E_2 & 0 \\ 0 & 0 & \bar{G} \end{bmatrix} \begin{Bmatrix} \epsilon_1 \\ \epsilon_2 \\ \gamma_{12} \end{Bmatrix} \qquad (3\text{-}3)$$

where the shear modulus, $\bar{G}$, is given by

$$\bar{G} = 1/4 \left[E_1 + E_2 \right] \qquad (3\text{-}4)$$

Previous researchers have related this shear modulus in the cracked state to only the tensile strains [5 and 16] in a completely empirical fashion. A review of the literature on this topic is continuing to determine if a more rational expression for the shear modulus can be obtained. Also, the influence and importance of the shear modulus on the load-displacement relations of masonry components will be investigated.

The material matrices in the principal strain directions are transformed into the local element global coordinates and combined with those for the reinforcement. Gauss point stresses are then calculated from the combined material matrices. Residual forces at the nodes are used in the iterative solution, and convergence is based on the ratio of the norm of the total residual forces at all nodes to the norm of the total external applied forces.

The material models for the masonry, reinforcement, and the composite reinforced overlay element are described in the following subsections. The sign convention used in the equations assume that strains and stresses in tension are positive and those in compression are negative.

3.3 MASONRY COMPRESSION MODEL

The material behavior in compression is described by a set of stress-strain relations and unloading rules. The stress-strain curve is based on the uniaxial properties of masonry prisms, and incorporates a strength reduction after tensile cracking normal to the principal compressive strains [27] and a strength increase due to lateral compressive confinement [18]. The stress-strain relations for masonry in compression are described by two second-order polynomials and an exponential tail as shown in Figure 3-1, and they are defined by the following equations:

$$f(\epsilon) = f_m \left[A_1(\epsilon/\epsilon_o) - \lambda\,(A_1-1)(\epsilon/\epsilon_o)^2 \right] \quad ; \quad 0 \geq \epsilon \geq \epsilon_p \qquad (3\text{-}5)$$

$$f(\epsilon) = f_p \left[1 - \frac{(\epsilon - \epsilon_p)^2}{(A_2\epsilon_o - \epsilon_p)^2} \right] \quad ; \quad \epsilon_p \geq \epsilon \geq \epsilon_e \qquad (3\text{-}6)$$

$$f(\epsilon) = f_e \left[A_3' + (1 - A_3') \exp\left[-\gamma \frac{(\epsilon - \epsilon_e)}{\epsilon_e} \right] \right] \quad ; \quad \epsilon < \epsilon_e \qquad (3\text{-}7)$$

where,

$f(\epsilon)$ = Principal compressive stress in the masonry.
ϵ = Principal compressive strain in the masonry.
f_m = Uniaxial compressive strength of the masonry.
ϵ_o = Strain at uniaxial compressive strength, f_m.
f_p = Peak uniaxial compressive strength of the masonry.
ϵ_p = Strain at peak uniaxial compressive strength, f_p.
λ = Strength modification factor.
ϵ_e = Point of tangency between Equations 3-6 and 3-7.
f_e = Compressive stress at point of tangency, ϵ_e.

γ = Exponential parameter

A_1 = Shape factor for the rising branch.

A_2 = Shape factor for the initial falling branch.

A_3' = Shape factor for the exponential falling branch.

A_3 = Shape factor or lower limit for the exponential falling branch.

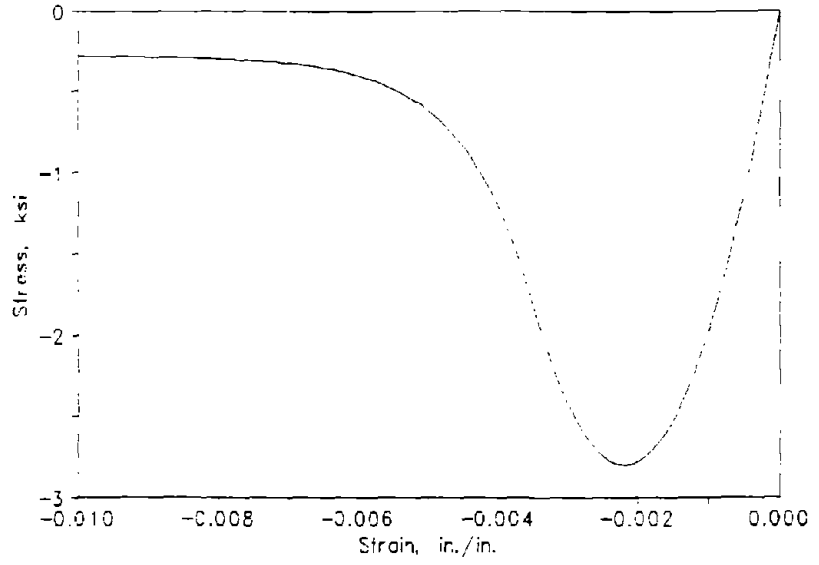

Figure 3-1. Compression Model for Masonry.

The lower limit of the exponential branch of Equation 3-7 is controlled by A_3 where,

$$f(\epsilon = \infty) = A_3 \, f_m \tag{3-8}$$

A_3' is determined by equating Equation 3-7 evaluated at $\epsilon = \infty$ and Equation 3-8 as given below:

$$f(\epsilon = \infty) = A_3' \, f_e = A_3 \, f_m \tag{3-7a}$$

$$A_3' = A_3(f_m/f_e) \tag{3-9}$$

The strength modification factor can account for a strength reduction after tensile cracking normal to the principal compressive strains [27] or a strength increase due to lateral compressive confinement [18]. Prior to any strength modification ($\lambda = 1$) the peak uniaxial compressive strength, f_p, and the strain at peak strength, ϵ_p, are equal to f_m and ϵ_o, respectively. After a strength modification they are functions of λ as given by the following equations:

$$\epsilon_p = \epsilon_o/\lambda \tag{3-10}$$

$$f_p = f_m/\lambda \tag{3-11}$$

The exponential tail (Equation 3-7) is attached to Equation 3-6 at ϵ_e as determined by the following equation:

$$\epsilon_e = \epsilon_o \left[1 + A_4(A_2-1)/\lambda \right] \tag{3-12}$$

where A_4 is a shape factor for the attachment point of the exponential tail. The exponential parameter, γ, is determined so that Equation 3-7 is tangent to Equation 3-6 at ϵ_e, and is given by:

$$\gamma = \frac{2f_m}{\lambda f_e} \frac{\epsilon_e}{(1-A_3')} \frac{(\epsilon_e - \epsilon_p)}{(A_2\epsilon_o - \epsilon_p)^2} \tag{3-13}$$

It can be seen that the stress-strain characteristics of the masonry in compression are determined by 6 parameters: f_m, ϵ_o, A_1, A_2, A_3, and A_4. The strength modification factor, λ, is determined from the state of principal stress and strain. The values of the shape factors used in Figure 3-1 are: $A_1 = 2$, $A_2 = 2$, $A_3 = 0.1$, and $A_4 = 0.6$. A_1 controls the shape of the rising branch and its value can range from 1.0 to 2.0, where $A_1 = 1.0$ gives a straight line from the origin to the peak strength and $A_1 = 2.0$ gives a second order polynomial tangent at the peak strength. Figure 3-2 shows variations in A_1 of 1.0, 1.25, 1.5, 1.75, and 2.0 ($A_2 = 2$, $A_3 = 0.1$, and $A_4 = 0.6$). A_2 controls the shape of the initial falling branch and its value can be greater than or equal to 1.0. Figure 3-3 shows variations in A_2 of 1.2, 1.4, 1.6, 1.8, and 2.0 ($A_1 = 2$, $A_3 = 0.1$, and $A_4 = 0.6$). A_4 controls the location of the attachment point of the

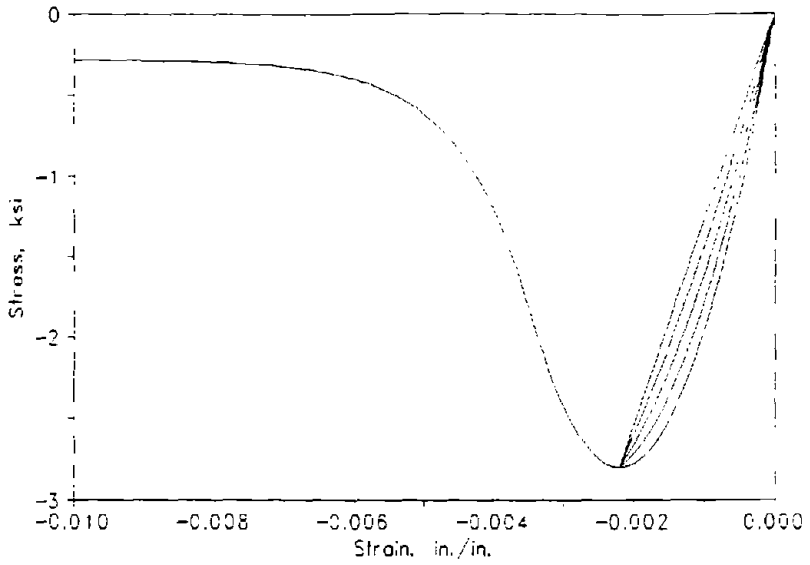

Figure 3-2. Compression Model Showing Variations in Shape Factor A_1 (A_1 = 1, 1.25, 1.5, 1.75, & 2).

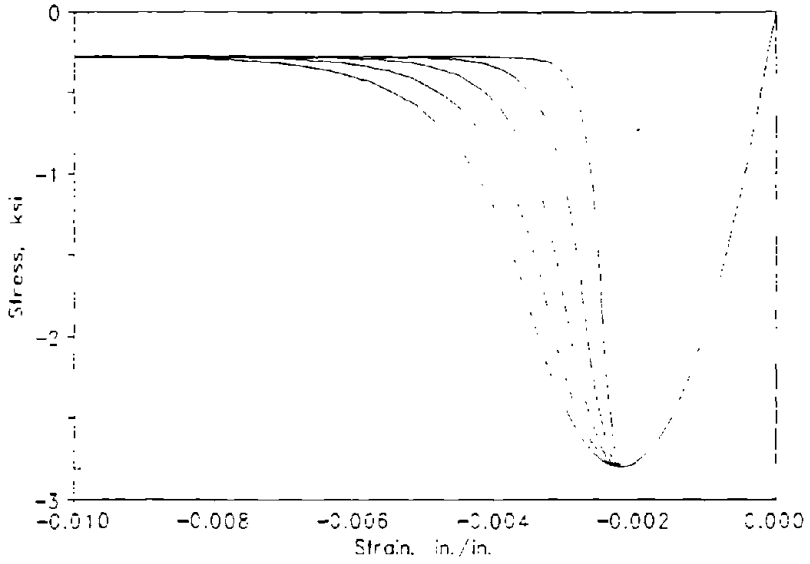

Figure 3-3. Compression Model Showing Variations in Shape Factor A_2 (A_2 = 1.2, 1.4, 1.6, 1.8, & 2.0).

exponential tail to the initial falling branch. Figure 3-4 shows variations in A_4 of 0.2, 0.3, 0.4, 0.5, and 0.6 (A_1 = 2, A_2 = 2, and A_3 = 0.1). A_3 controls the lower limit of the exponential falling branch and its value can range from 0.0 to less than 1.0. Figure 3-5 shows variations in A_3 of 0.1, 0.15, 0.2, 0.25, and 0.3 (A_1 = 2, A_2 = 2, and A_4 = 0.6). These parameters are compatible with the research and experimental testing by Atkinson and Kingsley [3], Hart et al [13], and Kingsley et al [17].

The model can accommodate the special case given by Hart et al [13] and Sajjad [24], where the initial falling branch is not used. In this case the compression model is described by a second-order polynomial for the rising branch and an exponential tail for the falling branch [13 and 24]. This model is obtained when A_2 = 1.0, and the exponential parameter γ is specified as A_4. Figure 3-6 shows this type of model where three curves presented by Hart et al [13] are given; namely, Unreinforced Masonry (URM), Spiral Type 2 confinement (SP2), and Wire Mesh Type 2 confinement (OWM2). However, it should be noted that Hart et al shows normalized curves while those given in Figure 3-6 have assumed values for f_m and ϵ_o.

A compressive strength reduction occurs after tensile cracking normal to the principal compressive strain, and in this case the strength modification factor, λ, is replaced by a damage parameter, β. The damage parameter is based on reinforced concrete research [27] and has been modified by others [16] as given below:

$$\beta = 1.0 \quad ; \quad \epsilon_t/\epsilon_c \geq -0.556 \qquad (3\text{-}14)$$

$$\beta = 0.85 - 0.27\,[\epsilon_t/\epsilon_c] \quad ; \quad -0.556 \geq \epsilon_t/\epsilon_c \geq -20.0 \qquad (3\text{-}15)$$

$$\beta = 6.25 \quad ; \quad \epsilon_t/\epsilon_c \leq -20.0 \qquad (3\text{-}16)$$

where ϵ_t/ϵ_c is the ratio of the principal normal tensile strain in the masonry to the principal compressive strain. Figure 3-7 shows β as a function of ϵ_t/ϵ_c. These relationships for β need to be modified for reinforced masonry, and this modification will be part of the next phase of this research work. Figure 3-8 shows some typical curves for strength reduction that occurs after normal tensile

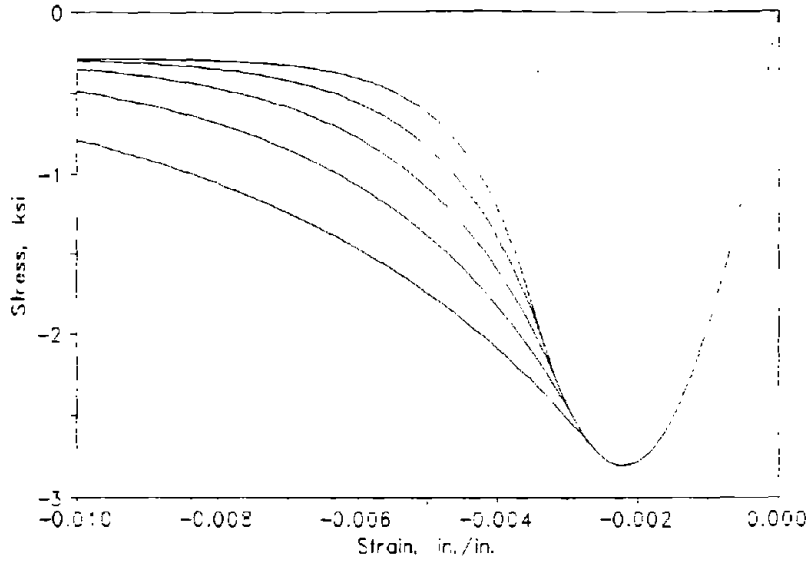

Figure 3-4. Compression Model Showing Variations in Shape Factor A_4 (A_4 = 0.2, 0.3, 0.4, 0.5, & 0.6).

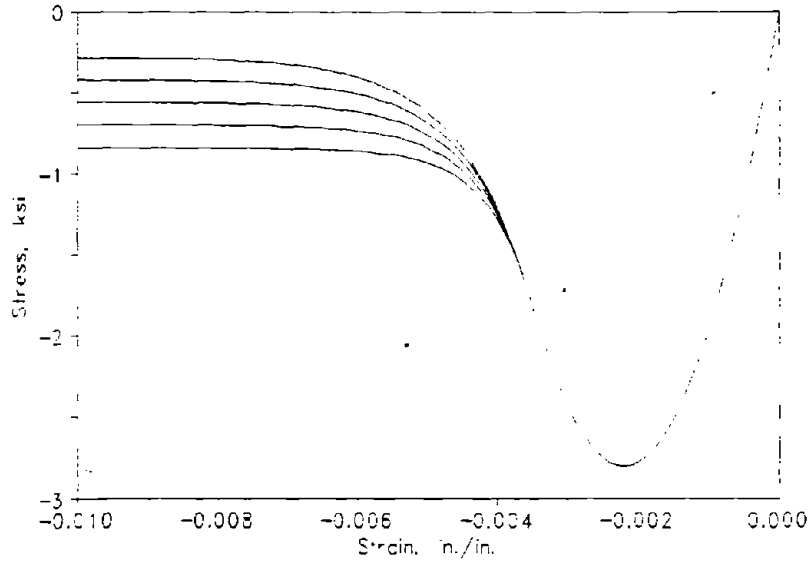

Figure 3-5. Compression Model Showing Variations in Shape Factor A_3 (A_3 = 0.1, 0.15, 0.2, 0.25, & 0.3).

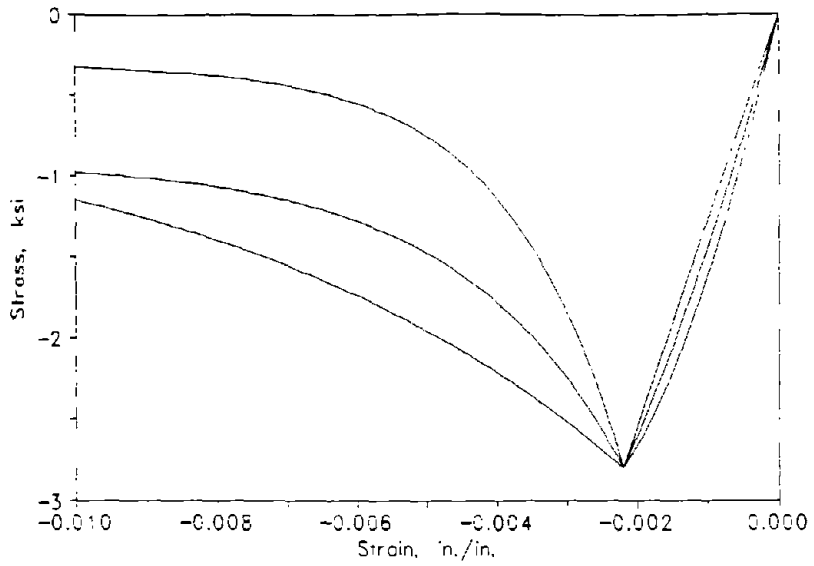

Figure 3-6. Compression Model Showing the Special Case with $A_2 = 1$, Model by Hart et al [13].

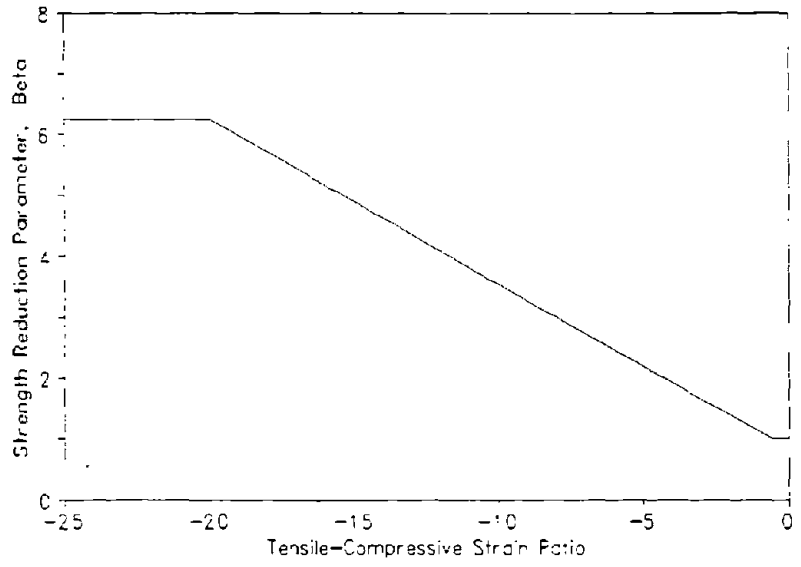

Figure 3-7. Compressive Strength Reduction Factor, β [27 & 16].

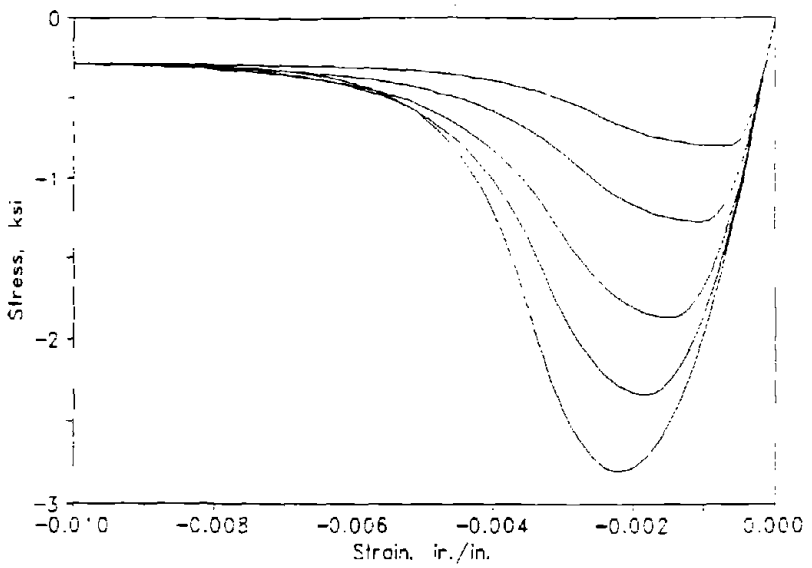

Figure 3-8. Compression Model Showing Strength Reductions for Various Values of β.

cracking. These curves are a function of the damage parameter, β, and the values of β used in the figure are 1.0, 1.2, 1.5, 2.2, and 3.5.

A compressive strength increase occurs when both principal stresses are compressive, and in this case the reciprocal of the strength modification factor, $1/\lambda$, is replaced by an enhancement parameter, η. The enhancement parameter is derived from concrete research by Kupfer et al [18] and it relates the compressive strength increase in principal direction 1 due to a compressive stress in principal direction 2 as given below:

$$\eta = 1/\lambda = \frac{(1 + A_5 \, f_2/f_1)}{(1 + f_2/f_c)^2} \quad ; \quad 0 \le f_2/f_1 \le 1 \qquad (3\text{-}17)$$

where f_1 and f_2 are the compressive stresses in principal directions 1 and 2, respectively, and A_5 is a constant. Concrete strength testing suggests a value for A_5 of 3.65 and this value may need to be modified for reinforced masonry. Figure 3-9 shows the enhancement parameter, η, due to lateral compressive

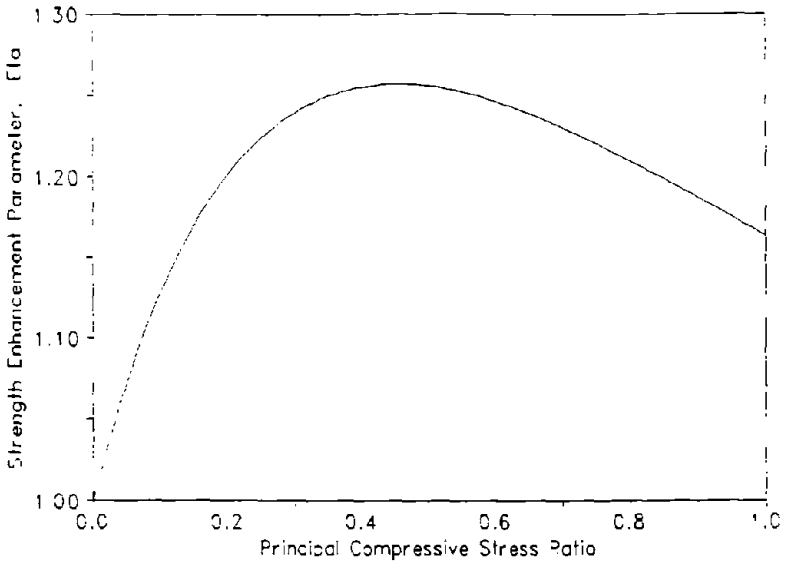

Figure 3-9. Compressive Strength Enhancement Factor, η.

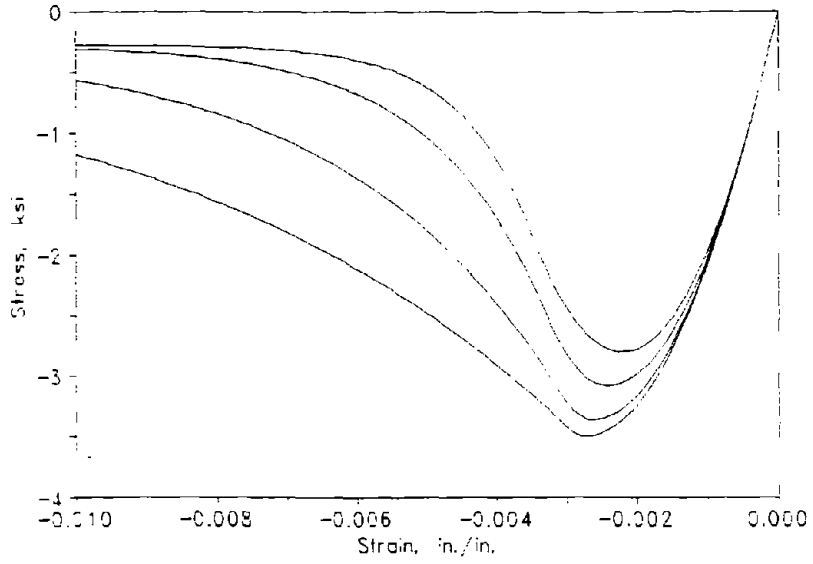

Figure 3-10. Compression Model Showing Strength Increases for Various Values of η.

confinement as a function of f_2/f_1. Figure 3-10 shows some typical curves for the strength increase that occurs due to lateral compressive confinement. These curves are a function of the strength enhancement parameter, η, and the values of η used in the figure are 1.0, 1.1, 1.2, and 1.25.

Unloading and reloading in compression follows a degrading modulus, E_u, that is defined by a line connecting the starting point of unloading on the envelope curve (e.g., point A) and a fixed focal point [28]. Figure 3-11 shows some typical degrading unloading paths, where the focal point is defined by the plus sign. It can be seen from the figure that all unloading paths are directed towards the focal point. The unloading modulus is given by

$$E_u = \frac{\sigma_A + A_6 \, f_p}{\epsilon_A + A_5 \, f_p/E_c} \tag{3-18}$$

where σ_A and ϵ_A are the stress and strain corresponding to the starting point of unloading on the envelope curve (e.g., point A), A_6 is the focal point factor,

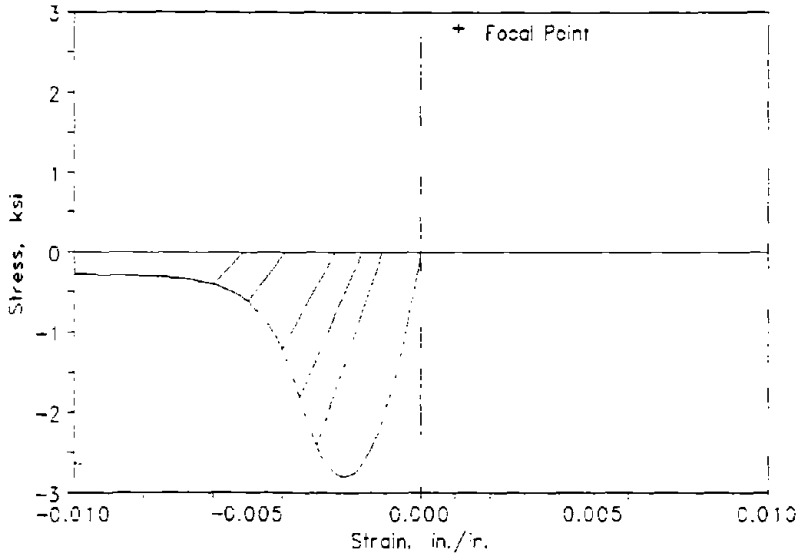

Figure 3-11. Typical Unloading Paths for Compression Model.

$A_6\ f_p$ is the focal point stress, and E_c is the initial compression modulus at $\epsilon = 0$. This modulus defines the residual or plastic strain, ϵ_u (i.e., the intersection of the unloading modulus and the stress axis). The residual or plastic strain is given by

$$\epsilon_u = \frac{A_6\ f_p\ \epsilon_A - A_6\ f_p\ \sigma_A/E_c}{A_6\ f_p + \sigma_A} \qquad (3\text{-}18a)$$

Concrete testing suggests a value for A_6 of 1.0 [28].

3.4 TENSION STIFFENING MODELS

Three models are included in the program to account for the tension stiffening effect in the composite overlay element of masonry and reinforcement. They include Model 1 - Unreinforced Masonry (i.e., no tension stiffening), Model 2 - Reinforced Masonry (an exponential decay model), and Model 3 - Reinforced Concrete (Vecchio and Collins [27]). These models are described in the following paragraphs.

Tension Stiffening Model 1 - Unreinforced Masonry, No Tension Stiffening. The stress-strain relations for Tension Stiffening Model 1 are shown in Figure 3-12 and are defined by the following equations:

$$f(\epsilon) = E_t\ \epsilon_t \quad ; \quad 0 \le \epsilon_t \le \epsilon_{cr} \qquad (3\text{-}19)$$

$$f(\epsilon) = 0 \quad ; \quad \epsilon_t > \epsilon_{cr} \qquad (3\text{-}20)$$

where,

$f(\epsilon)$ = Stress in the masonry due to tension stiffening.
E_t = Modulus of elasticity of the masonry in tension.
ϵ_t = Tensile strain in the masonry.
ϵ_{cr} = Tensile cracking strain of the masonry.

This model is intended to be used in the regions of the masonry that are unreinforced.

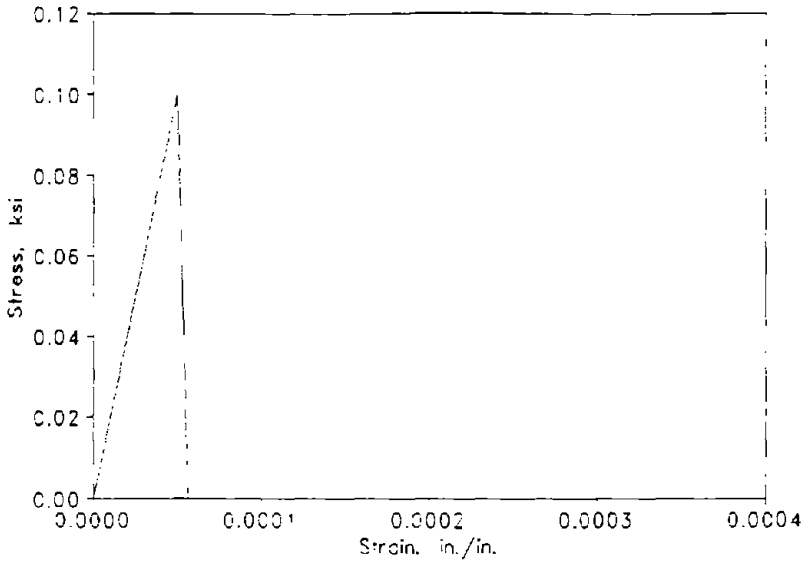

Figure 3-12. Tension Stiffening Model 1, Unreinforced Masonry.

Tension Stiffening Model 2 - Reinforced Masonry, Exponential Decay Model. The stress-strain relations for the exponential tension stiffening model are shown in Figure 3-13 and are defined by the following equations:

$$f(\epsilon) = E_t \, \epsilon_t \qquad ; \quad 0 \le \epsilon_t \le \epsilon_{cr} \qquad (3\text{-}21)$$

$$f(\epsilon) = f_{cr} \left[B_1 + (1 - B_1) \exp \left[-\alpha \, \frac{(\epsilon_t - \epsilon_{cr})}{\epsilon_{cr}} \right] \right] \; ; \quad \epsilon_t > \epsilon_{cr} \qquad (3\text{-}22)$$

where,

$f(\epsilon)$ = Stress in the masonry due to tension stiffening.

E_t = Modulus of elasticity of the masonry in tension.

ϵ_t = Tensile strain in the masonry.

ϵ_{cr} = Tensile cracking strain of the masonry.

f_{cr} = Tensile cracking stress of the masonry.

α = Positive exponential parameter.

B_1 = Lower limit for the exponential branch.

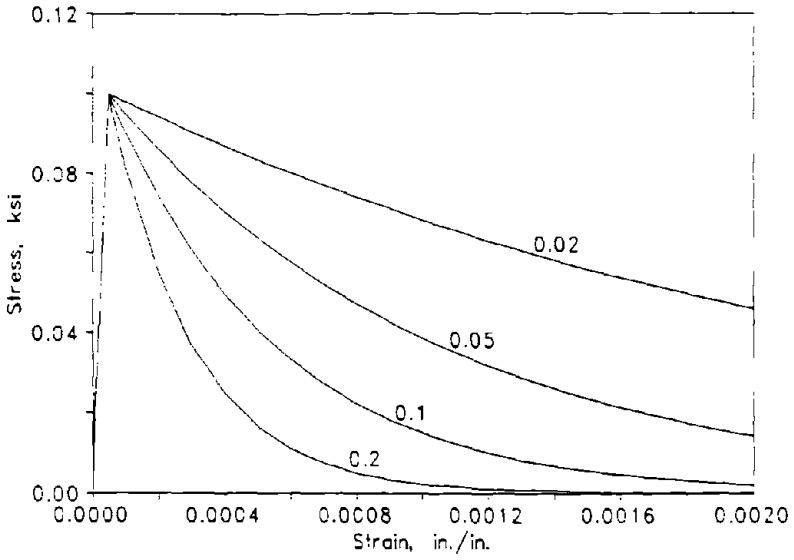

Figure 3-13. Tension Stiffening Model 2, Reinforced Masonry, Exponential Decay Model.

The lower limit for the exponential branch, B_1, was incorporated in the model as suggested by Hegemier [14]. Figure 3-13 shows the shape of the tension stiffening model for four typical values of the exponential parameter, α (0.02, 0.05, 0.1, & 0.2), where $B_1 = 0$. The exponential parameter, α, is related to the percentage of reinforcement, ρ [12 and 19], and its value increases as the reinforcement percentage increases. Figure 3-14 shows suggested curves for 4 values of ρ (0.25, 0.35, 0.50, & 0.75%). The values used for α and B_1 in Figure 3-14 are given in Table A-2 in Appendix A. These curves are based on the research by Gupta et al [12] and are in general agreement with his simplified model for strains that are below the yield of the reinforcement. The models by Gupta et al [12] and others reduce the tension stiffening stress to zero when yielding of the reinforcement is approached (i.e., the combined tension stiffening stress plus the reinforcement stress can not exceed the yield stress of the reinforcement). The current model includes a provision to reduce the tension stiffening stress to zero at the reinforcement yield strain.

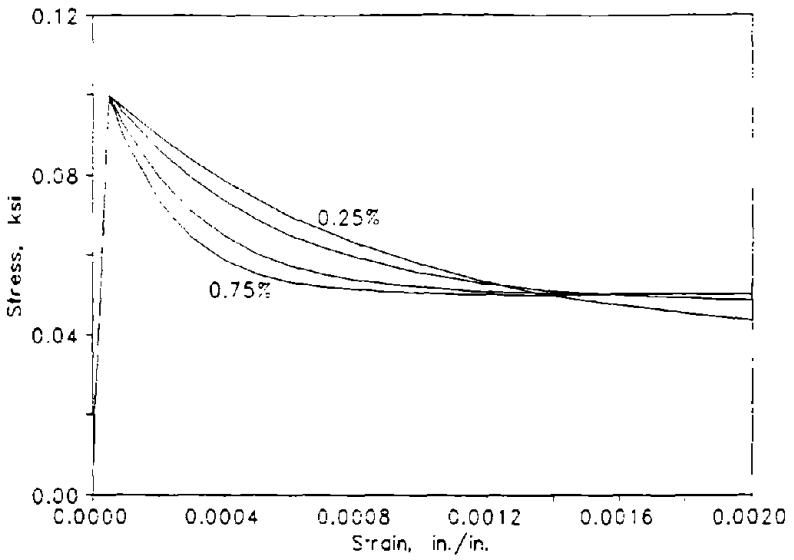

Figure 3-14. Tension Stiffening Model 2, Reinforced Masonry, Suggested Curves for ρ = 0.25, 0.35, 0.50, & 0.75%.

Tension Stiffening Model 3 - Reinforced Concrete (Vecchio and Collins). The stress-strain relations for Tension Stiffening Model 3 are shown in Figure 3-15 and are defined by the following equations:

$$f(\epsilon) = E_t \, \epsilon_t \qquad ; \quad 0 \leq \epsilon_t \leq \epsilon_{cr} \tag{3-23}$$

$$f(\epsilon) = \frac{f_{cr}}{1 + (200\epsilon_t)^{\frac{1}{3}}} \qquad ; \quad \epsilon_t > \epsilon_{cr} \tag{3-24}$$

This model was developed by Vecchio and Collins [27] for use in reinforced concrete and may not be appropriate for reinforced masonry.

Unloading in Tension - Unloading and reloading in tension follows a degrading modulus that is defined by a line connecting the starting point of unloading on the envelope curve and the tension origin or toe (i.e., a secant modulus). This cyclic load path corresponds to the opening and closing of the tensile cracks.

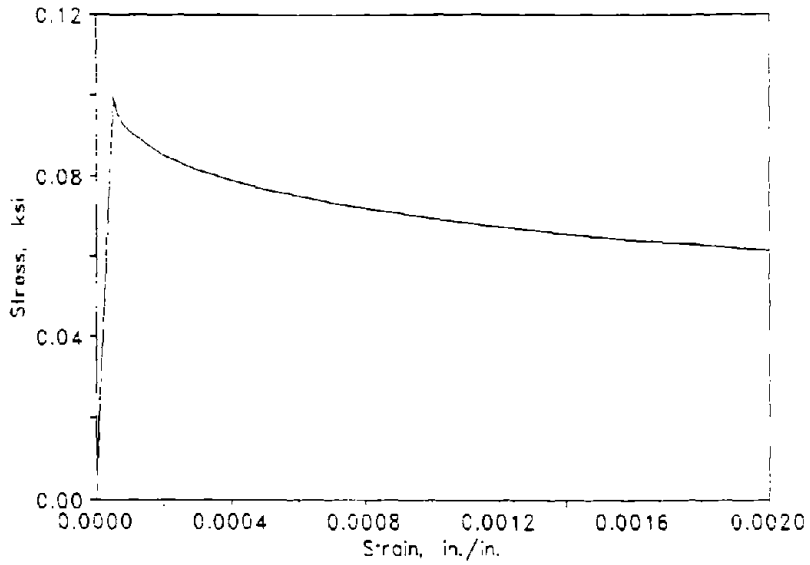

Figure 3-15. Tension Stiffening Model 3, Reinforced Concrete (Vecchio and Collins) [27].

3.5 BIMODULAR MASONRY MODEL

The masonry model envelope curve for tensile and compressive strains is shown in Figure 3-16, where the effects of the compression model (Figure 3-1) and the tension stiffening model (Figure 3-13) are combined. This model retains all of the behavior characteristics and features described earlier for the compression and tension models, including loading, unloading, and reloading. It can be seen from Figure 3-16 that the masonry material model is bimodular with different properties in tension and compression.

A typical cyclic path for the masonry model is shown in Figure 3-17 overlaid with the envelope curve. The tension stress-strain curve remains attached to the compression stress-strain curve and the tensile strains are determined from the point of attachment.

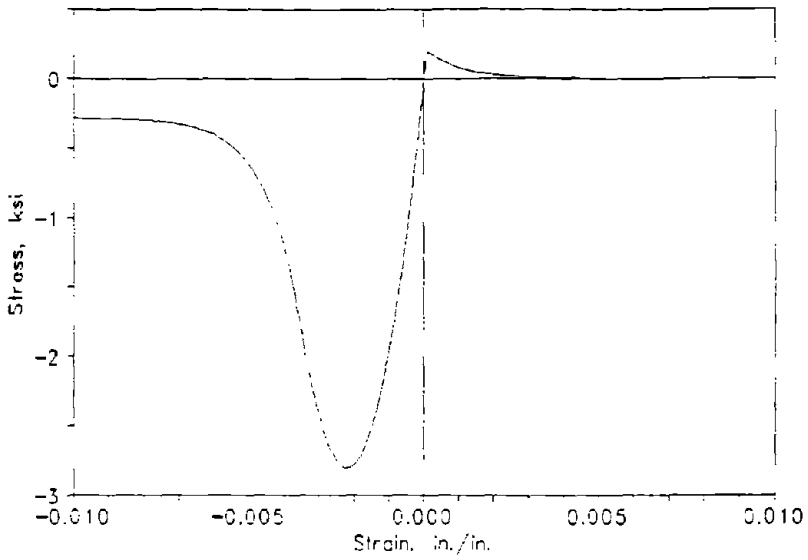

Figure 3-16. Masonry Model, Tension and Compression.

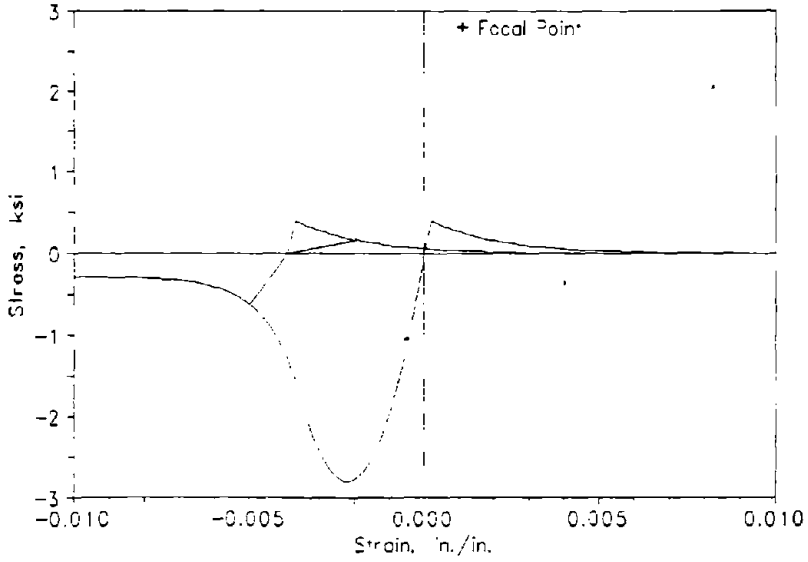

Figure 3-17. Masonry Model, Typical Cyclic Load Path.

3.6 REINFORCEMENT MODEL

The reinforcing steel is represented by a bilinear model as shown in Figure 3-18. This model has been shown to adequately represent the yielding that is expected to occur in typical masonry walls and panels, especially for the short gauge lengths provided by the tensile cracks. The plastic modulus is given by

$$E_{sp} = E_s \left[1 - \frac{E_s}{E_s + H'} \right] \tag{3-25}$$

or alternately,

$$E_{sp} = \zeta E_s \tag{3-26}$$

where,

E_{sp} = Plastic modulus of the reinforcement.
E_s = Modulus of elasticity of the reinforcement.
H' = Strain-hardening parameter.
ζ = Bilinear factor.

The hardening parameter is determined by

$$H' = \frac{\zeta E_s}{(1 - \zeta)} \tag{3-27}$$

Unloading and reloading between the parallel softening / plastic branches (i.e., branches defined by stiffness E_{sp}) occurs along the larger initial stiffness E_s. When a loading cycle raises the effective tensile yield point (e.g., loading from the origin to point 1 in Figure 3-18), a corresponding reduction in the effective compressive yield point is produced, and conversely. This is called the Bauschinger effect. A typical unloading / reloading path is shown in Figure 3-18. Unloading begins at point 1 on the plastic branch and follows stiffness E_s to point 2, the new effective compressive yield point. Unloading then follows stiffness E_{sp} to point 3. Reloading follows stiffness E_s to point 4. It can be seen that this type of unloading and reloading results in a hysteretic behavior.

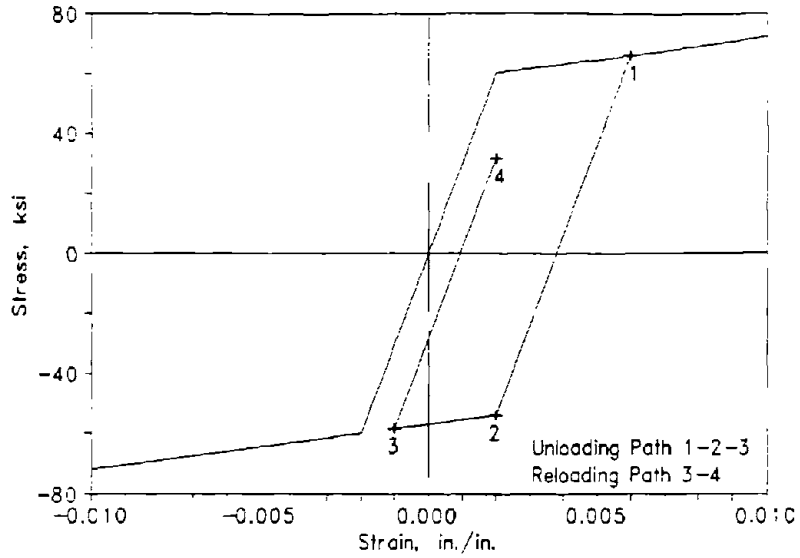

Figure 3-18. Reinforcement Model.

3.7 REINFORCED MASONRY ELEMENT MODEL

The reinforced masonry model for tensile and compressive strains is shown in Figure 3-19, where the contributions of the masonry model (Figure 3-16) are combined with those of the reinforcement model (Figure 3-18). It can be seen from Figure 3-19 that the bimodular characteristics of the masonry material model are retained in the reinforced masonry material model.

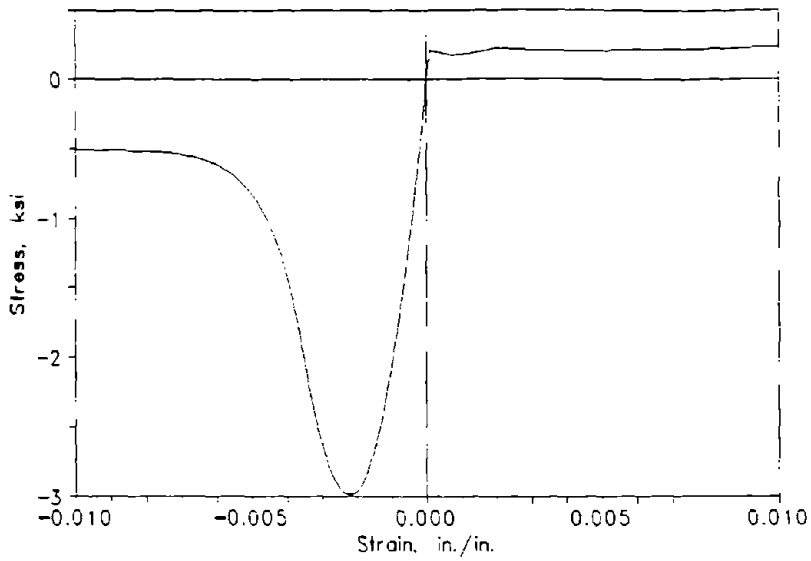

Figure 3-19. Reinforced Masonry Model, Masonry and Reinforcement.

SECTION 4

ANALYTICAL METHOD AND COMPUTATIONAL ALGORITHM

4.1 INTRODUCTION AND INTENDED USE

The development of a nonlinear finite element model for the analysis of reinforced masonry or reinforced concrete structures involves the selection and formulation of appropriate analytical models and computational algorithms and the programming of a computer code or program that incorporates these models and algorithms. The analytical model must exhibit the phenomenological behavior observed in reinforced masonry and concrete, and it must employ physical properties that are representative of these materials. A detailed description of the developed phenomenological models and their constitutive properties is given in Section 3 and a general description of the computer code is given in Section 2. The computational algorithm and solution strategy for the nonlinear finite element model is given in this section.

The finite element model developed in this project is intended to be used in the prediction of and correlation with experimental results obtained from one-story walls tested at the University of Colorado, two-story walls tested at the University of Texas at Austin, three-story walls and a five-story building tested at the University of California, San Diego [25]. The masonry walls in these experiments are tested under in-plane cyclic loading. The model will be used to correlate with and predict the envelope of the hysteretic loops using monotonic loading, and it will be capable of cyclic unloading for one or more complete cycles. Since these walls are subjected to inelastic displacements, the model will be able to handle strain softening behavior of the masonry.

4.2 FORMULATION OF THE ANALYTICAL METHOD AND COMPUTATIONAL ALGORITHM

The FEM/I computer program uses the isoparametric finite element with 4, 8, and 9 nodes as its base element. This element has been thoroughly tested and has been shown to work very well [6, 15, and 29]. The 4, 8, and 9 node element is used for elastic models and the 4 node element is used for the nonlinear model. The analytical method and computational algorithm selected for the nonlinear

model is influenced by several requirements and capabilities that are needed for the analysis of reinforced masonry components. This has been accomplished by providing:

- a model that accounts for the post-peak compressive and tensile strength behavior.
- the capability to simulate crushing in the compression toe.
- degrading unloading rules for the material models.
- the capability for monotonic and cyclic loading.
- the capability to calculate component force-deflection envelopes beyond their peak strength (i.e., passing over limit points).
- a formulation that avoids the negative stiffness associated with strain softening behavior.
- a model that converges when the mesh size is reduced.
- positive and reasonably rapid convergence.
- computational efficiency to control the computer time required to obtain a solution.

A direct iteration method is computationally expensive since the stiffness matrix needs to be computed and inverted in every iteration of each load increment. Another difficulty with the direct iteration method is that unloading could lead to negative stiffnesses and cause divergence of the solution process. A tangent stiffness method cannot handle the negative stiffness associated with strain softening, and the method diverges when passing over limit points because of the zero stiffness. An initial stiffness method with applied loading diverges near the limit points, since an additional load increment near the peak strength could exceed the ultimate strength capacity. The initial stiffness approach has been avoided by other researchers due to these types of problems [4].

An approach that avoids the above difficulties employs the initial stiffness method, where applied incremental displacements are the primary excitation [23 and 30]. In this approach, the initial stiffness is used throughout the solution and the stiffness matrix needs to be inverted only once at the start of the solution process. This approach converges for models with strain softening and models with degrading unloading rules, and when passing over limit points [21].

4.3 COMPUTATIONAL ALGORITHM AND SOLUTION STRATEGY

The program uses an initial stiffness formulation with an incremental solution method, where displacements and/or forces can be used as the primary excitation. This method is a straightforward computational strategy and is reliably convergent for softening systems when prescribed displacements are used as the primary excitation. The selected computation algorithm is an incremental one, where the displacements and/or loads are applied incrementally and iterative corrections are performed in every increment to bring the nonlinear system into equilibrium. The computational procedure is best described by defining the sequence of steps that are involved in the solution process. These steps are given in the following paragraphs.

Step 1 - Calculate an initial stiffness using the material properties of the element components in the initial stages of loading. Assuming that the initial material modulus for the masonry is the same in tension and compression, the initial stiffness is calculated using the following material matrix at the Gauss points of each element:

$$D_m = \frac{E_m}{1 - \nu^2} \begin{bmatrix} 1 & \nu & 0 \\ \nu & 1 & 0 \\ 0 & 0 & (1-\nu)/2 \end{bmatrix} + \begin{bmatrix} \rho_{sh} E_s & 0 & 0 \\ 0 & \rho_{sv} E_s & 0 \\ 0 & 0 & 0 \end{bmatrix} \qquad (4\text{-}1)$$

where,

E_m = Initial elastic modulus of masonry.

ν = Poisson's ratio of masonry.

E_s = Elastic modulus of reinforcement.

ρ_{sh} = Reinforcement ratio in the horizontal direction.

ρ_{sv} = Reinforcement ratio in the vertical direction.

Step 2 - Apply a load increment composed of displacements and/or forces. An incremental force can be used if limit points are not to be passed.

Step 3 - Calculate the incremental and total nodal point displacements. At nodes where displacements are prescribed, reactions are computed. The set of equations to be solved in iteration i is as follows:

$$[K^{o}] \quad \{\Delta U\}^{(i)} = \{\Delta F\}^{(i)} \tag{4-2}$$

where,

$[K^{o}]$ = Assembled initial stiffness matrix.

$\{\Delta U\}^{(i)}$ = Incremental displacement at iteration i.

$\{\Delta F\}^{(i)}$ = Incremental forces. These forces take on different values depending on the iteration number, as described below:

- 1^{st} iteration - Incremental applied force vector for the current load step plus the residual force vector $\{\Delta R\}^{(i)}$ from the previous iteration.
- Subsequent iterations - Residual force vector from the previous iteration.

The residual force vector $\{\Delta R\}^{(i)}$ is a measure of the load imbalance between the external loads and the internal resistance in the system at the i^{th} iteration.

Step 4 - Evaluate the total strains at the Gauss points. These values are obtained using the following relations:

$$\{\epsilon\}^{(i)} = [B] \quad \{U\}^{(i)} \tag{4-3}$$

where,

$\{\epsilon\}^{(i)}$ = Total strains at the Gauss point in the i^{th} iteration (ϵ_x, ϵ_y, γ_{xy}).

$[B]$ = Strain-displacement matrix evaluated numerically at the Gauss points.

Step 5 - Evaluate the principal total strains at the Gauss points using the total strains computed in the step above. In this step the principal strains, ϵ_1 and ϵ_2, and the direction of principal axis x_1 (θ) are determined.

Step 6 - Compute the orthotropic secant moduli E_1 and E_2 in the principal directions x_1 and x_2. The moduli E_1 and E_2 are determined from the compressive stress-strain relations or the tensile stress-strain relations (tension stiffening model) depending on whether ϵ_1 and ϵ_2 are tensile or compressive strains. These values are computed at the Gauss points.

Step 7 - Form a secant material matrix for the masonry at the Gauss points, using the secant material moduli E_1 and E_2. This matrix is based on two different constitutive laws, one for the uncracked case and one for the cracked case. Before tensile cracking, the constitutive law follows the Darwin and Pecknold model [7] as given below:

$$\begin{Bmatrix} \sigma_1 \\ \sigma_2 \\ \tau_{12} \end{Bmatrix} = \frac{1}{1 - \nu^2} \begin{bmatrix} E_1 & \nu(E_1E_2)^{\frac{1}{2}} & 0 \\ \nu(E_1E_2)^{\frac{1}{2}} & E_2 & 0 \\ 0 & 0 & \bar{G} \end{bmatrix} \begin{Bmatrix} \epsilon_1 \\ \epsilon_2 \\ \gamma_{12} \end{Bmatrix} \qquad (4\text{-}4)$$

where,

$$\bar{G} = 1/4 \left[E_1 + E_2 - 2\nu(E_1E_2)^{\frac{1}{2}} \right] \qquad (4\text{-}5)$$

After tensile cracking, the constitutive law for the masonry is given by a diagonal matrix as given below:

$$\begin{Bmatrix} \sigma_1 \\ \sigma_2 \\ \tau_{12} \end{Bmatrix} = \begin{bmatrix} E_1 & 0 & 0 \\ 0 & E_2 & 0 \\ 0 & 0 & \bar{G} \end{bmatrix} \begin{Bmatrix} \epsilon_1 \\ \epsilon_2 \\ \gamma_{12} \end{Bmatrix} \qquad (4\text{-}6)$$

where,

$$\bar{G} = 1/4 \left[E_1 + E_2 \right] \qquad (4\text{-}6a)$$

$\bar{G}$ is the shear modulus that has a diminishing value due to tensile strains. At the current stage of the research, this shear modulus is given by Equation 4-6a.

where E_1 and E_2 are the secant moduli in the x_1 and x_2 directions corresponding to ϵ_1 and ϵ_2. Previous researchers have related this shear modulus in the cracked state to only the tensile strains [5 and 16] in a completely empirical fashion. A review of the literature on this topic is continuing in order to determine if a more rational expression for the shear modulus can be obtained. Also, the influence and importance of the shear modulus on the load-displacement relations of masonry components will be investigated.

Step 8 - Transform the material matrix for the masonry component from the orthotropic coordinates into the local element coordinates. The transformed material matrix is computed as follows:

$$[D_m]^{(i)} = [T]^T [\bar{D}_m] [T] \tag{4-7}$$

where $[\bar{D}_m]$ is the material matrix of the masonry in the orthotropic directions as determined in Step 7. The transformation matrix [T] can be shown to take the following form:

$$[T] = \begin{bmatrix} c^2 & s^2 & cs \\ s^2 & c^2 & -cs \\ -2cs & 2cs & c^2-s^2 \end{bmatrix} \tag{4-8}$$

where $c = \cos \theta$, $s = \sin \theta$, and θ is the angle between the x-axis and the principal axis x_1.

Step 9 - Evaluate the secant material matrix for the reinforcement component. This matrix is based on the strain values in the x- and y- directions since the steel is assumed to behave in a uniaxial fashion. This matrix takes the following form:

$$[D_s]^{(i)} = \begin{bmatrix} \rho_{sh} E_{sx} & 0 & 0 \\ 0 & \rho_{sh} E_{sy} & 0 \\ 0 & 0 & 0 \end{bmatrix} \tag{4-9}$$

where E_{sx} and E_{sy} are the secant material moduli for the steel reinforcement in the x- and y-directions, respectively. They are determined from the following expressions:

$$E_{sx} = E_s \quad ; \quad \epsilon_x < \bar{\epsilon}_{yx} \tag{4-10}$$

$$E_{sx} = [\, E_s \, \bar{\epsilon}_{yx} + E_{sp} \, (\epsilon_x - \bar{\epsilon}_{yx}) \,]/\epsilon_x \quad ; \quad \epsilon_x \geq \bar{\epsilon}_{yx} \tag{4-11}$$

$$E_{sy} = E_s \quad ; \quad \epsilon_y < \bar{\epsilon}_{yy} \tag{4-12}$$

$$E_{sy} = [\, E_s \, \epsilon_y + E_{sp} \, (\epsilon_y - \bar{\epsilon}_{yy}) \,]/\epsilon_y \quad ; \quad \epsilon_y \geq \bar{\epsilon}_{yy} \tag{4-13}$$

where E_{sp} is the plastic moduli of the steel reinforcement, and $\bar{\epsilon}_{yx}$ and $\bar{\epsilon}_{yy}$ are the yield strains in the reinforcement in the x- and y-directions, respectively.

Step 10 - A combined material matrix based on the strain states at the Gauss points is obtained by combining the matrices for the two components. This approach is based on the assumption that the two components share the same nodal point strains. Thus, the combined material matrix is as follows:

$$[D]^{(i)} = [D_m]^{(i)} + [D_s]^{(i)} \tag{4-14}$$

Step 11 - The true stresses at the Gauss points are computed using the secant material matrix constructed in previous steps.

$$\{\sigma\}^{(i)} = [D]^{(i)} \, \{\epsilon\}^{(i)} \tag{4-15}$$

where $\{\sigma\}^{(i)}$ and $\{\epsilon\}^{(i)}$ are the total stress and strain vectors at the Gauss points.

Step 12 - Calculate the residual force vector, which is a measure of load imbalance between external forces and internal resistance forces. This vector is computed as follows:

$$\{\Delta R\}^{(i)} = \{R\}^{(i)} - \int_v [B]^T \{\sigma\}^{(i)} dV \tag{4-16}$$

where $\{\Delta R\}^{(i)}$ is the residual force vector. $\{R\}^{(i)}$ is the external force vector at iteration i, which contains the reactions at nodal points with prescribed displacement and the residual forces from the last iteration. The second expression on the right hand side of the equation is a measure of internal forces due to true stresses.

Step 13 - The next step is to check convergence of the iterative solution process. A convergence criterion can be based on either nodal displacement or on residual forces [23]. A criterion based on residual forces was selected and is defined as follows:

$$\lambda^2 = \frac{\sum_{j=1}^{N} (\Delta R_j^{(i)})^2}{\sum_{j=1}^{N} (R_j^{(i)})^2} \qquad (4\text{-}17)$$

where,

$\Delta R_j^{(i)}$ = Unbalanced residual force at node j and iteration i.

$R_j^{(i)}$ = Total external applied force at node j and iteration i.

N = Total number of nodal points.

λ = A convergence tolerance parameter. Ratio of the norm of the unbalanced residual forces to the norm of the total applied forces.

The convergence tolerance is selected by the user. However, a value of 1 to 2 percent is found to be satisfactory for this class of problems.

The FEM/I code has three criteria for the unbalanced residual force that are used to exit from the iteration loops; namely,

- Convergence - Termination with convergence (*normal termination*) occurs when the ratio of the norm of the unbalanced residual forces to the norm of the total applied forces is less than or equal to a prescribed percentage or prescribed convergence tolerance.

- Iterations - Termination before reaching convergence (*premature termination*) can occur when the maximum number of iterations are exceeded.
- Slow convergence - Termination before reaching convergence (*premature termination*) can also occur when the difference between the ratio of the norm of the unbalanced residual forces to the norm of the total applied forces in successive iterations is less than a specified fraction of the prescribed convergence tolerance. The program defaults can be modified to adjust this specified fraction or to omit the check on slow convergence altogether.

Step 14 - If the convergence criteria are not met, the external force vector is updated and the solution is iterated. If the convergence criteria are met, the loads are incremented and the solution process is continued.

The discussion given above does not include some formulation details that are readily available in the literature. For example; shape functions for specific elements, isoparametric transformations, equation solution schemes, local to global transformations for stress vectors, etc. are not presented in this report.

SECTION 5

DEFINITION OF INPUT DATA

5.1 INTRODUCTION

The FEM computer code is comprised of two separate but integrated processors; namely,

- FEM-CALC is the calculation and solution processor.
- FEM-POST is a postprocessor. (Under development)

The computer programs are coded in FORTRAN 77 and are operational on IBM compatible personal computers, such as the 286/386/486 systems and the PC/AT. The programs are compiled using the Ryan-McFarland RM/FORTRAN compiler, Version 2.44, and the Lahey F77L FORTRAN compiler, Version 5.0. They can also be compiled using the MicroSoft FORTRAN compiler, Version 5.0. A version that will run in extended memory on 486 systems will be available when the research is completed. This version will be compiled under the Lahey F77L-EM32 FORTRAN compiler, Version 4.0, and linked with Lahey/Ergo OS/386. The postprocessor is not required to run the main calculation and solution processor. It is provided to enhance the user interface with the main program by providing tools for displaying the calculated results for data interpretation.

The executable elements of the programs are:

FEM.EXE for the main calculation processor
POST.EXE for the postprocessor. (Under development)

This section describes the operation of the FEM computer code and the input data required by the main calculation processor.

5.2 FEM-CALC - Calculation and Solution Processor

The main calculation and solution processor performs the linear or nonlinear, incremental, static analysis of finite element models of reinforced masonry and concrete building systems and components. The definition of the required input data for the calculation and solution processor of the FEM computer program is presented in this section. The input is organized in 19 card groups. Any system of units can be used, but the input data must be in a consistent set of units.

The following pages present the content and format of the 19 card groups. All the input data are in free format, except for alphanumeric strings. The input data must be entered into a formatted ASCII file, and the file can be prepared with almost any available text editor. The input filename must conform to the rules for DOS file specifications, and is comprised of a filename with up to eight (8) characters and an optional extension with up to three (3) characters (i.e., Nnnnnnnn.Eee).

Although the executable element, FEM.EXE, can be stored anywhere in the directory system, execution of the program must be initiated from the directory where the input data file is stored. Execution of the program is initiated by using a batch file similar to the one provided with the program, **FEM-EXE**. The batch file **FEM-EXE** should be modified to reflect the directory structure of the user's computer system. Upon execution, the program displays the computer program name and version identification line, and then requests the file specification or name of the input file (e.g., Nnnnnnnn.Eee = Wall-03a.Inp). The input file name is to be entered as shown below:

```
------------------------------------------------
 Program                  F E M / I   Ver. 105
------------------------------------------------
Enter name of the Input file ..... Wall-03a.Inp
```

The computer program can produce as many as five (5) output files. The program automatically names these output files using the filename portion of the input file specification (e.g., Nnnnnnnn = Wall-03a) and appends a three (3) character extension to identify the output file as shown below:

```
-----------------------------------------------
 Program                  F E M / I   Ver. 105
-----------------------------------------------
Enter name of the Input file ..... Wall-03a.Inp
The Output File Name is .......... Wall-03a.Out
The Postprocessor File Name is ... Wall-03a.Pst
The Force-Deflection File Name is. Wall-03a.Fdf
The Major Event File Name is ..... Wall-03a.Mef
The Restart File Name is ......... Wall-03a.Rst
```

Output files with the .Out and .Mef extensions are always generated, whereas the files with the .Pst, .Fdf, and .Rst extensions are only generated at the request of the user through the input data.

The program produces several information and status displays as the program continues its execution. The user does not need to attend the run after the input file name has been provided. The program can also be run in an unattended batch mode. All output is directed to the file names listed and is available to the user after the run has been completed.

The definition of the required input data for the 19 card groups of the FEM calculation and solution processor computer program is given on the following pages. The definition provided is for Version 105 of the computer program. Differences in the definition of the input data for earlier versions are given in Appendix C.

Appendix A gives an analysis model that is intended to demonstrate the use of the FEM/I computer program and to serve as a guide for the preparation of the input data for a typical application.

Card Group 1	Program Execution Option	
No. of Records	1	
Format	A8	
Variable	**Description**	**Notes**
OPTION	Program execution option (Columns 1-8). = START^^^ (^ denotes a blank) Read input for a new problem. **Go to Card Group 2.** = RESTART^ (^ denotes a blank) Restart of a previous problem from a file. **Go to Card Group 19.**	

Card Group 2	Problem Title	
No. of Records	1	
Format	A80	
Variable	**Description**	**Notes**
JOBHED	Problem TITLE, limited to 80 alphanumeric characters (Columns 1-80). **Go to Card Group 3.**	

Card Group 3	Problem Control Parameters	
No. of Records	1	
Format	Free Field	
Variable	**Description**	**Notes**
NPOIN	Total number of nodal points.	
NELEM	Total number of elements.	
NVFIX	Total number of constrained nodal points, where one or more degrees of freedom are restrained or have prescribed displacements.	
NTYPE	Problem type parameter. = 1, Plane stress = 2, Plane strain = 3, Axisymmetric	
NNODE	Number of nodes per element. = 4, Linear quadrilateral element = 8, Quadratic quadrilateral element = 9, Quadratic quadrilateral element	
NMATS	Total number of different materials.	
INISR	Initial stress parameter. = 0, No initial stress = 1, Initial stresses generated from linear distribution given in Card Group 8. = 2, Initial stresses read from a file. = 3, Initial stresses to be written to an initial stress file.	
IPFLAG	Postprocessor parameter. = 0, A postprocessor file is not generated. = 1, A postprocessor file is generated as specified in Card Group 18.	
IREST	Restart parameter. = 0, A restart file is not generated at the end of the run. = 1, A restart file is generated at the end of the run. Go to Card Group 4.	

Card Group 4	Element Data	
No. of Records	NELEM	
Format	Free Field	
Variable	**Description**	**Notes**
NUMEL	Element number.	(1)
MATNO	Material property number.	
LNODS(1)	1st Nodal connectivity number (K_1).	(2,3)
LNODS(2)	2nd Nodal connectivity number (K_2).	(2,3)
...	...	
LNODS(N)	Nth Nodal connectivity number (K_N).	(2,3)
	Go to Card Group 5.	

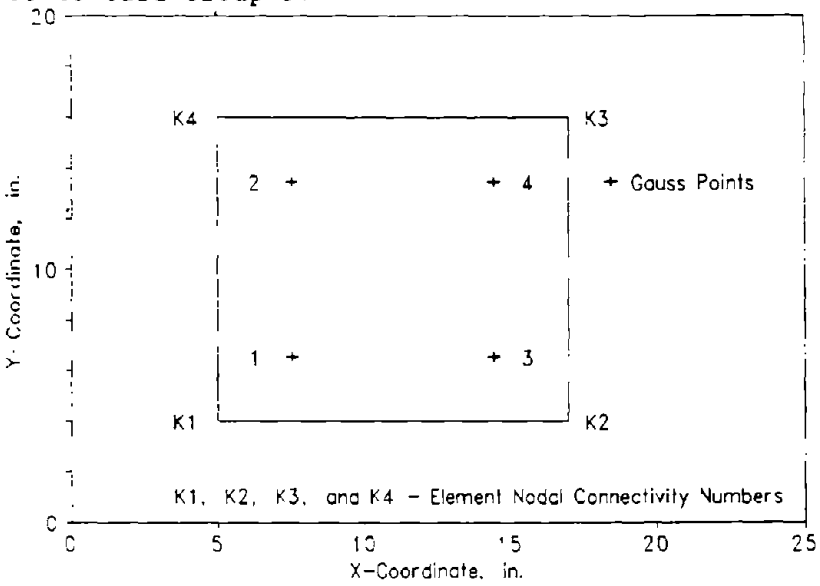

NOTES:

(1) Element data can be input in any order.

(2) Specify N = NNODE connectivity numbers.

(3) The nodal connectivity numbers must be listed in a counterclockwise sequence, starting from any corner node. The location of the Gauss points relative to the element nodal connectivity numbers is shown in the figure above. Specifying the element nodal connectivity numbers by starting at the same corner of each element (e.g., lower left hand corner) in the mesh guarantees that the Gauss points of all of the elements will be located in the same relative position. This is invaluable in the interpretation of the element stresses and strains.

Card Group 5	Nodal Point Data	
No. of Records	Variable (1,2,3)	
Format	Free Field	
Variable	**Description**	**Notes**
IPOIN	Nodal point number.	(3,4)
COORD(1)	x (or r) coordinate of the node.	
COORD(2)	y (or z) coordinate of the node.	
	Go to Card Group 6.	
NOTES:		
(1)	The total number of records in this card group may be less than or equal to NPOIN. For quadratic elements (NNODE = 8 or 9) with straight sides, it is only necessary to specify data for the corner nodes, and the coordinates of the intermediate mid-side nodes will be automatically interpolated.	
(2)	Do not input the coordinates of the 9th (central) node for Lagrangian elements (NNODE = 9).	
(3)	This card group is terminated when the coordinates of the NPOINth node are input.	
(4)	The coordinates of the highest numbered node must be input regardless of whether it is a midside node or not.	

Card Group 6	Constrained Node Data	
No. of Records	NVFIX	
Format	Free Field	
Variable	**Description**	**Notes**
NOFIX	Constrained node number.	(1)
IFPRE	Constraint code: = 10, Nodal displacement constraint in the x (or r) direction. = 01, Nodal displacement constraint in the y (or z) direction. = 11, Nodal displacement constraint in both coordinate directions.	
PRESC(1)	The prescribed value of the x (or r) component of nodal displacement.	(2)
PRESC(2)	The prescribed value of the y (or z) component of nodal displacement.	(2)
	Go to Card Group 7.	
NOTES:		
(1)	Constrained node numbers must be given in ascending order.	
(2)	The prescribed displacements are invoked when the node is constrained in the corresponding degree of freedom. The prescribed displacement values are multiplied by a factor that is defined at each loading increment (Card Group 18).	

Card Group 7	Material Property Data	
No. of Records	NMATS Sets	
Format	Free Field	
Variable	**Description**	**Notes**
	Record 1 Material ID	
NUMAT	Material identification number.	
MATID	Material identification description (60 characters max.) enclosed with apostrophes (e.g., 'Masonry').	
	Record 2 - n Material Properties	(1)
	General Properties	
PR(1) - ν	Poisson's ratio of the masonry, ν.	
PR(2) - t	Element thickness, t. Zero for axisymmetric problems.	
PR(3) - ρ	Weight density per unit volume of the composite, ρ.	
PR(4) - MMN	Material Model No., MMN. = 0, Elastic model. = 1, Nonlinear reinforced masonry model.	
	Compressive Properties	
PR(5) - f_m	Uniaxial compressive strength of masonry, f_m.	
PR(6) - ϵ_o	Masonry strain at uniaxial compressive strength, ϵ_o.	
PR(7) - A_1	Shape factor for the rising branch, A_1.	
PR(8) - A_2	Shape factor for the initial falling branch, A_2.	
PR(9) - A_3	Shape factor or lower limit for the exponential falling branch, A_3.	
PR(10) - A_4	Shape factor for the attachment point of the exponential tail, A_4.	
PR(11) - MCD	Compression Damage Parameter Model No., MCD. = 1, Use β from Equations (3-14, 3-15, & 3-16). = 2, β = 1.0.	
	Continued	

Card Group 7	Material Property Data (Concluded)	
No. of Records	NMATS Sets	
Format	Free Field	
Variable	**Description**	**Notes**
	Record 2 - n Material Properties (Concluded)	(1)
	Tensile Properties	
PR(12) - f_{cr}	Tensile cracking strength of masonry, f_{cr}.	
PR(13) - E_t	Elastic modulus of the masonry in tension, E_t.	
PR(14) - MTS	Tension Stiffening (TS) Model No., MTS.	
PR(15) - B_1	Lower limit of the exponential branch for TS Model No. 2, B_1.	
PR(16) - α	Exponential parameter α (positive) for TS Model No. 2.	
	Reinforcement Properties	
PR(17) - E_s	Elastic modulus of the reinforcement, E_s.	
PR(18) - ζ	Bilinear factor for the plastic modulus, E_{sp}, of the reinforcement, $\zeta = E_{sp}/E_s$.	
PR(19) - ρ_v	Vertical reinforcement ratio, ρ_v.	
PR(20) - ρ_h	Horizontal reinforcement ratio, ρ_h.	
PR(21) - f_{yv}	Yield stress of the vertical reinforcement, f_{yv}.	
PR(22) - f_{yh}	Yield stress of the horizontal reinforcement, f_{yh}.	
	Go to Card Group 8.	
NOTES:		
(1)	All 22 material properties must be supplied; and since the values are input in free field format, the number of records will depend on how the user enters the data.	

Card Group 8	Initial Stress Data	
No. of Records	1 (1)	
Format	Free Field	
Variable	**Description**	**Notes**
YI	Elevation of the point at which the initial stress $\sigma(o)$ is specified.	
GRD	Vertical gradient of the stress.	
STRESI(1)	σ_x^o or σ_r^o (plane or axisymmetric).	
STRESI(2)	σ_y^o or σ_z^o (plane or axisymmetric).	
STRESI(3)	σ_{xy}^o or σ_{rz}^o (plane or axisymmetric).	
STRESI(4)	σ_z^o or σ_θ^o (plane or axisymmetric).	
	Go to Card Group 9.	
NOTES:		
(1)	Required if INISR=1, otherwise skip this card group.	

Card Group 9	Output Control Parameters	
No. of Records	Variable (2)	
Format	Free Field	
Variable	**Description**	**Notes**
	Record 1 Control Parameters	
NSELM	Number of elements for which printed stress and strain output is desired (see Card Group 10).	
NSNOD	Number of nodes for which printed displacement output is desired (see Card Group 11).	
NUMFDF	Number of nodes in the constrained node set (i.e., Card Group 6) that define the reactions and deflection to be output to the force-deflection file (maximum of 20).	(1)
	Record 2 Optional Control Parameters	(2)
KOMPNT	Component of the reaction and deflection to be output. = 1, x direction = 2, y direction	
NODE1	Node number whose reaction is to be included in the force-deflection file.	(3)
...	...	
...	...	
NODEn	Node number whose reaction is to be included in the force-deflection file.	(3)
	Go to Card Group 10.	
NOTES:		
(1)	A force-deflection file can be created that includes a component of the displacement at a specific node and the sum of the reaction forces at a series of related nodes, where all the nodes must have prescribed displacement as defined in Card Group 6.	
(2)	Record 2 is required when NUMFDF is greater than 0.	
(3)	The displacement output to the force-deflection file is the displacement of NODE1. The force output to the file is the sum of the reactions at NODE1 through NODEn. NUMFDF entries must be provided.	

Card Group 10	Element Output Control Data	
No. of Records	Variable (1)	
Format	Free Field	
Variable	**Description**	**Notes**
ISNEL(1)	Number of the first element selected for printed stress and strain output.	(2)
...	...	
...	...	
ISNEL(N)	Number of the last element selected for printed stress and strain output. **Go to Card Group 11.**	(2)
NOTES:		
(1)	Required if NSELM > 0 and NSELM < NELEM, otherwise skip this card group. If printed stress and strain output is not required for any elements, then set NSELM = 0 and skip this card group. If printed stress and strain output is required for all elements, then set NSELM = NELEM and skip this card group. If printed stress and strain output is required for NSELM elements where 0 < NSELM < NELEM, then this card group is required to define the desired element numbers.	
(2)	NSELM elements must be provided and the element numbers must be given in ascending order.	

Card Group 11	Node Output Control Data	
No. of Records	Variable (1)	
Format	Free Field	
Variable	**Description**	**Notes**
ISNOD(1)	Number of the first node selected for printed displacement output.	(2)
...	...	
...	...	
ISNOD(N)	Number of the last node selected for printed displacement output.	(2)
	Go to Card Group 12.	
NOTES:		
(1)	Required if NSNOD > 0 and NSNOD < NPOIN, otherwise skip this card group. If printed displacement output is not required for any nodal points, then set NSNOD = 0 and skip this card group. If printed displacement output is required for all nodal points, then set NSNOD = NPOIN and skip this card group. If printed displacement output is required for NSNOD nodal points where 0 < NSNOD < NPOIN, then this card group is required to define the desired nodal point numbers.	
(2)	NSNOD nodes must be provided and the node numbers must be given in ascending order.	

Card Group 12	Load Case Title	
No. of Records	1	
Format	A80	
Variable	**Description**	**Notes**
TITLE	Title of the load case, limited to 80 alphanumeric characters (Columns 1-80). **Go to Card Group 13.**	

Card Group 13	Applied Load Control Data	
No. of Records	1	
Format	Free Field	
Variable	**Description**	**Notes**
IPLOD	Nodal point load control parameter. = 0, No concentrated nodal point loads to be input. = 1, Concentrated nodal point loads to be input.	
IGRAV	Gravity loading control parameter. = 0, No gravity loading to be input. = 1, Gravity loading to be input.	
IEDGL	Edge loading control parameter. = 0, No distributed edge loads to be input. = 1, Distributed edge loads to be input. Go to Card Group 14.	

Card Group 14	Nodal Point Loads	
No. of Records	Variable (1)	
Format	Free Field	
Variable	**Description**	**Notes**
LODPT	Node number.	(2)
POINT(1)	Load component in x (or r) direction.	(3)
POINT(2)	Load component in y (or z) direction.	(3)
	Go to Card Group 15.	
NOTES:		
(1)	Required if IPLOD = 1, otherwise skip this card group.	
(2)	The last card must be that for the highest numbered node (NPOIN) whether it is loaded or not.	
(3)	For axisymmetric problems, the loads input should be the total loading on the circumferential ring passing through the nodal point concerned.	

Card Group 15	Gravity Loading	
No. of Records	1 (1)	
Format	Free Field	
Variable	**Description**	**Notes**
THETA	Angle in degrees of the gravity axis measured counterclockwise from the negative vertical direction defined by the y (or z) axis, $0 < \theta < 180$.	
GRAVY	Gravitational acceleration factor that is applied to the material weight density per unit volume, ρ, for the calculation of the gravity loading. The weight density is defined by PR(3) in Card Group 7. The gravity loading is determined by GRAVY * ρ * Element Volume. Go to Card Group 16.	
NOTES:		
(1)	Required if IGRAV = 1, otherwise skip this card group.	

Card Group 16	Edge Loading Control	
No. of Records	1 (1)	
Format	Free Field	
Variable	**Description**	**Notes**
NEDGE	Number of element edges on which distributed loads are to be applied. **Go to Card Group 17.**	
NOTES:		
(1)	Required if IEDGL = 1, otherwise skip this card group and Card Group 17.	

Card Group 17	Edge Loading	
No. of Records	Variable (1,2)	
Format	Free Field	
Variable	**Description**	**Notes**
	Record 1 Element Faces for Edge Loading	(2)
NEASS	Number of the element that has a distributed edge loading.	
NOPRS(1)	Nodal point numbers that define the loaded edge of the element. The nodal point numbers must be given in a counterclockwise sequence.	
NOPRS(2)	Same as above.	
NOPRS(3)	Same as above.	(3)
	Record 2 Distributed Loads for Edge Loading	(2,4)
PRES(1,1)	Value of normal component of distributed load at node NOPRS(1).	
PRES(1,2)	Value of tangential component of distributed load at node NOPRS(1).	
PRES(2,1)	Value of normal component of distributed load at node NOPRS(2).	
PRES(2,2)	Value of tangential component of distributed load at node NOPRS(2).	
PRES(3,1)	Value of normal component of distributed load at node NOPRS(3).	(3)
PRES(3,2)	Value of tangential component of distributed load at node NOPRS(3).	(3)
	Continued	

Card Group 17	Edge Loading (Concluded)	
No. of Records	Variable (1,2)	
Format	Free Field	
Variable	**Description**	**Notes**
	Go to Card Group 18.	
NOTES:		
(1)	Required if IEDGL = 1, otherwise skip this card group.	
(2)	Records 1 and 2 must be repeated in turn for every element edge that has a distributed load. The element edges can be input in any order.	
(3)	For linear four node elements, • omit PRES(3,1) and PRES(3,2) and • omit NOPRS(3).	
(4)	Distributed loads (i.e., loading per unit length) along an element edge can be applied in a normal and/or tangential direction. The nodal point numbers that define the loaded edge of the element must be given in a counterclockwise sequence. A distributed loading normal to an element edge is positive if it acts in a direction into the element. A distributed loading tangential to an element edge is positive if it acts in a counterclockwise direction along the element edge.	

Card Group 18	Load Increment Controls (1)	
No. of Records	Variable (2)	
Format	Free Field	
Variable	**Description**	**Notes**
NDIV	Number of divisions used to generate load increments between the loading levels defined on the preceding input data record in this card group and the loading levels defined by this input data record. - 1, The input data entries on this record define a single loading level to be reached in this load increment. No additional load increments are generated. - N, Generate N-1 load increments between the loading levels defined by the preceding and the current input data records. = -1, Terminate reading of the input data records in this card group. All other data entries on the last record are ignored.	(1,2)
FACTN	Factor for nodal point force loading. The total nodal point force loading at the current increment is equal to FACTN times the nodal point forces defined in Card Group 14. If NDIV > 1, the total nodal point force loading at each generated load increment is linearly interpolated between the values defined by the preceding and the current input data records of this card group.	(1)
FACTG	Factor for gravity loading. The total gravity loading at the current increment is equal to FACTG times the gravity forces defined in Card Group 15. If NDIV > 1, the total gravity loading at each generated load increment is linearly interpolated between the values defined by the preceding and the current input data records of this card group. Continued	(1)

Card Group 18	Load Increment Controls (1) (Continued)	
No. of Records	Variable (2)	
Format	Free Field	
Variable	**Description**	**Notes**
FACTE	Factor for edge loading. The total distributed edge loading at the current increment is equal to FACTE times the edge loads defined in Card Groups 16 and 17. If NDIV > 1, the total edge loading at each generated load increment is linearly interpolated between the values defined by the preceding and the current input data records in this card group.	(1)
FACTD	Factor for the prescribed displacements. Total prescribed displacement loading at the current increment is equal to FACTD times the prescribed displacements defined in Card Group 6. If NDIV > 1, the total prescribed displacement loading at each generated load increment is linearly interpolated between the prescribed displacement values defined by the preceding and the current input data records in this card group.	(1)
TOLER	Convergence tolerance factor, defined in percent (i.e., 1% = 1.0).	(3)
MITER	Maximum number of iterations allowed.	(3)
NOUTP	Printed output control flag. = 0, No output. = 1, Output displacements for this load increment only. = 2, Output displacements and reactions for this load increment only. = 3, Output displacements, reactions, and element stresses and strains for this load increment only. = 11, Same as 1, except output the results for all load increments generated by this input data record. = 12, Same as 2, except output the results for all load increments generated by this input data record. = 13, Same as 3, except output the results for all load increments generated by this input data record.	
	Continued	

Card Group 18	Load Increment Controls (1) (Continued)	
No. of Records	Variable (2)	
Format	Free Field	
Variable	**Description**	**Notes**
NALGO	Solution algorithm control parameter. Stiffness Matrix is Updated at: = 1, 1st Iteration of 1st Load Increment = 2, 1st Iteration of This Load Increment	(3)
NPLOT	Postprocessor file generation control flag. = 0, Do not write a postprocessor output response record for this load increment. = 1, Write a postprocessor output response record for this load increment only. = 11, Write a postprocessor output response record for all load increments generated by this input data record.	
NREST	Restart flag. = 0, Do not generate a restart file at the end of this load increment. = 1, Generate a restart file at the end of this load increment and terminate execution. = 2, Generate a restart file at the end of this load increment and continue execution. End of Input. Continued	(4)

Card Group 18	Load Increment Controls (1) (Concluded)	
No. of Records	Variable (2)	
Format	Free Field	
Variable	**Description**	**Notes**
NOTES:		
(1)	The loading for the finite element model is comprised of a combination of prescribed nodal point displacements, nodal point forces, gravity loads, and normal and tangential distributed edge loads, as defined in Card Groups 6 and 13 - 17, respectively. These loads are applied in incremental steps; and this card group defines the total number of increments in which the loading is to be applied, as well as the loading levels to be reached at each increment. For each input data record of this card group: • The values of FACTD, FACTN, FACTG, and FACTE in define the loading level to be reached. • The total prescribed displacements to be reached are defined by FACTD multiplied by the displacements given in Card Group 6. • The total applied forces are defined by FACTN, FACTG, and FACTE multiplied by the forces given in Card Groups 14, 15, and 16 & 17, respectively. • The value of NDIV defines the number of increments to be used to reach the prescribed loading levels. • NDIV = 1 defines a single load increment. • When NDIV > 1, additional load increments are generated. The total number of increments is defined by the summation of the values of NDIV given in all input data records.	
(2)	This card group is terminated when NDIV is set to a negative number. All data entries on the last data record are ignored.	
(3)	Invoked for all generated load increments.	
(4)	Invoked only on the last load increment.	

Card Group 19	Restart Controls	
No. of Records	1	
Format	Free Field	
Variable	**Description**	**Notes**
NINCS	Accumulated number of load increments applied in the previous computer runs from which the restart files were generated.	(1)
IPFLAG	Postprocessor file parameter. - 0, A postprocessor file is not generated. - 1, A postprocessor file is generated as specified in Card Group 18.	
IREST	Restart parameter. - 0, A restart file is not generated at the end of the run. - 1, A restart file is generated at the end of the run.	
	End of input.	

5.3 FEM-POST - Postprocessor

The postprocessor produces graphical displays of the results from the main calculation processor. This program is not required for the interpretation of the output from the main calculation processor, since the main calculation processor can produce extensive printed output. However, it provides the user with very useful tools for the analysis of calculated results. It can produce deformed meshes, principal stress and strain directions, crack orientations, and reinforcement responses.

The postprocessor is still under development as part of the ongoing TCCMAR Category 2 research, and is not being released with this version on the computer program.

SECTION 6

EXAMPLE APPLICATIONS

6.1 INTRODUCTION

The overall objective of example application problems is threefold; namely,

- Demonstration - Demonstrate the use of the computer program, so that new users will have a guide to the preparation of input for other applications.
- Verification - Verify that the solution algorithms, elements, and material models perform as formulated by the authors. The purpose is to determine if the program can faithfully replicate the intended performance under well defined conditions.
- Validation - Validate the computer program for use in the designed applications. The purpose is to determine if the program can be used to represent real physical applications. This is best accomplished by comparing a calculation (i.e., numerical simulation) with an experiment.

Demonstration Objective - The analysis model given in Appendix A is intended to demonstrate the use of the FEM/I computer program and to serve as a guide for the preparation of the input data for a typical application.

Verification Objective - Program verification was accomplished using a series of single element problems, where different states of strain were imposed on the element. The strain states included uniaxial and biaxial conditions. Each aspect of the material models were verified separately using this process before they were employed in a complete problem. These single element verification problems are not included in this report.

Validation Objective - The FEM/I computer code will be used in the TCCMAR program to analyze reinforced masonry building components and walls, since it is not feasible to conduct tests on all needed configurations. However, before it can be used to extrapolate beyond the types and configurations of components being tested, the computer program must first be verified and then validated by correlating the analytical results with experimental measurements. The example

applications given in this section satisfy part of the validation requirements. However, validation will continue throughout the experimental phase of the TCCMAR research; and the results of the validation process will be reported separately.

6.2 EXPERIMENTS ON ONE-STORY REINFORCED MASONRY WALLS

Quasi-static, cyclic tests on reinforced concrete masonry piers are being conducted at the University of Colorado as part of the TCCMAR research program [26]. These experiments provide a unique opportunity to validate the program by correlating the analytical results with experimental measurements.

6.2.1 Description of the Experiments

The wall panel specimens tested at the University of Colorado were 72 in. wide, 72 in. high, and 5 5/8 in. thick, and were fabricated with 6 x 8 x 16 in. hollow concrete block units. Bond beam units were used throughout, which allowed the grout to completely fill the head joints. The vertical and horizontal reinforcement was relatively uniformly distributed in both directions, and the walls were fully grouted. The horizontal reinforcement was anchored to the outside vertical reinforcement using 180-degree bend hooks. The walls were fabricated on a reinforced concrete base that was bolted to the laboratory floor, and were capped with a reinforced concrete top beam. The vertical reinforcement in the wall continued into both the top beam and the base, and was anchored using 180-degree bend hooks. The loading consisted of a constant vertical axial load and a lateral displacement loading sequence, where the axial load was applied at the beginning of the test and the lateral displacements were applied sequentially (i.e., displacement control). Both the axial loads and lateral displacements were applied by hydraulic actuators attached to a stiff steel beam member that was bolted to the concrete beam cast on top of the wall. The lateral loads were applied so that the resultant was at the top surface of the specimen.

6.2.2 Configurations Selected For Analysis

Six wall specimens from the fifteen that have been tested up to this point in the program were selected for correlation with FEM/I at this time. These specimens were selected because they represent configurations that display both flexure and shear response modes that are induced by their vertical and horizontal

reinforcement ratios and the applied axial load. They also show the effects of varying the axial load. The reinforcement characteristics and axial load data for the selected configurations are given in Table 6-1. Prism strengths were obtained from three-high unit prisms and ranged between 2600 and 3200 psi.

TABLE 6-1
Properties of the Walls Selected for Correlation.

Wall No.	Vertical Reinforcement				Horizontal Reinforcement				Axial Load psi
	Qty.	ρ_s %	f_y ksi	f_u ksi	Qty.	ρ_s %	f_y ksi	f_u ksi	
6	5 #5	0.38	64	103	5 #3	0.14	58	85	0
4	5 #7	0.74	71	103	5 #3	0.14	58	85	0
12	5 #5	0.38	64	104	5 #4	0.24	67	107	100
5	5 #7	0.74	71	103	5 #3	0.14	58	85	100
2	5 #5	0.38	64	103	9 #3	0.24	56	82	270
3	5 #7	0.74	74	111	5 #3	0.14	56	82	270

6.3 NONLINEAR FINITE ELEMENT ANALYSIS

The finite element mesh used in the analyses is shown in Figure 6-1. The pier is 72 in. sq. and is fabricated using 6 in. concrete blocks; and in addition to the wall, the model includes the concrete base and top member. The loading applied to the model was similar to that used in the test program, except that monotonic displacements were used instead of cyclic displacements. The constant vertical axial load was applied at the beginning of the calculation and the lateral displacements were applied sequentially (i.e., under displacement control).

The analytical correlations with the experiments are based on the overall lateral force-deflection envelope of the pier, as well as the sequence of major events including yielding of the reinforcement, masonry cracking, and masonry crushing.

The calculations were performed with Version 101 of the FEM/I program [9 and 10] (the first version), which did not have many of the material refinements that are included in this revision of the User's Guide. Properties for the analyses were taken directly from component tests conducted as part of the experimental program when available or they were estimated from prior research. The value for the uniaxial compressive strength was estimated from prism tests that showed some variability, where the data ranged from 2600 to 3200 psi. In addition to the values given in Table 6-1, the values used in the calculations included: a uniaxial compressive strength of 2900 psi, strain at peak strength of 0.0026 in./in., tensile cracking strength of 100 psi, masonry modulus of 2,900,000 psi, Poisson's ratio of 0.16, tension stiffening parameter that ranged from 0.02 to 0.04 for the reinforcement ratios used, and a reinforcement hardening parameter of 2%. Values for the damage factor, β, are not directly available from masonry testing. Although it is recognized that the values developed for reinforced concrete are not necessarily appropriate for reinforced masonry, they have been used in these calculations. Parametric studies will be conducted to determine appropriate values for determining β.

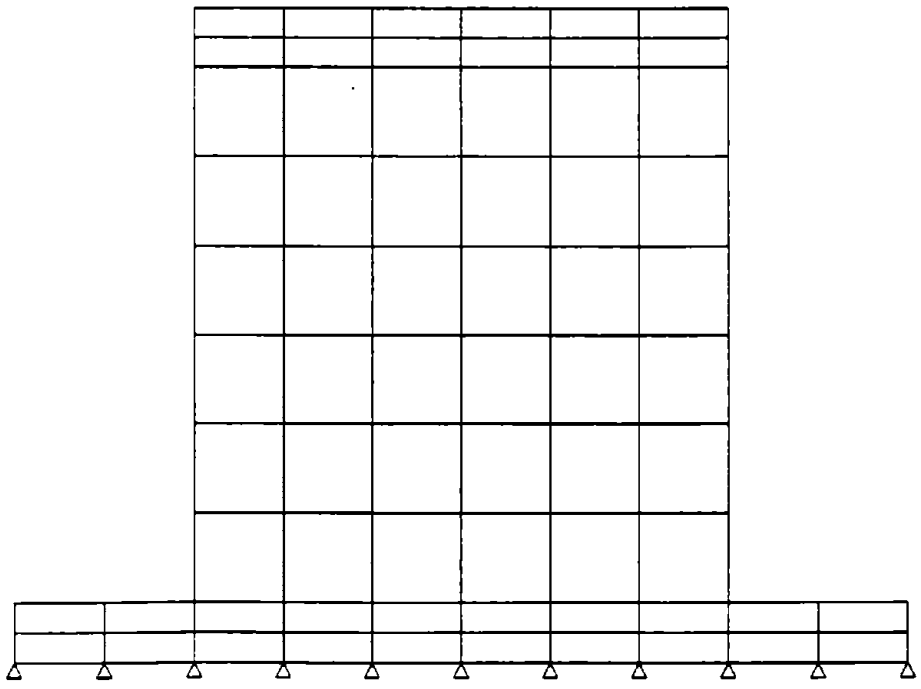

Figure 6-1. Finite Element Mesh For One-Story Reinforced Masonry Walls.

6.4 CORRELATION BETWEEN ANALYSIS AND EXPERIMENT

The cyclic test data taken from the experiments overlaid with monotonic envelope curves from the analyses are provided for each of the walls identified in Table 6-1. The data curves for Walls 6, 4, 12, 5, 2, and 3 are given in Figures 6-2 through 6-7, respectively. In addition, the peak lateral forces from the experiments and the analyses are tabulated in Table 6-2.

TABLE 6-2
Comparison of Peak Forces Between Experiments and Analyses.

Wall No.	Test Results		Analysis Peak Force Kips
	Positive Peak Force Kips	Negative Peak Force Kips	
6	52	48	57
4	72	87	94
12	71	71	72
5	89	84	104
2	83	98	95
3	100	105	117

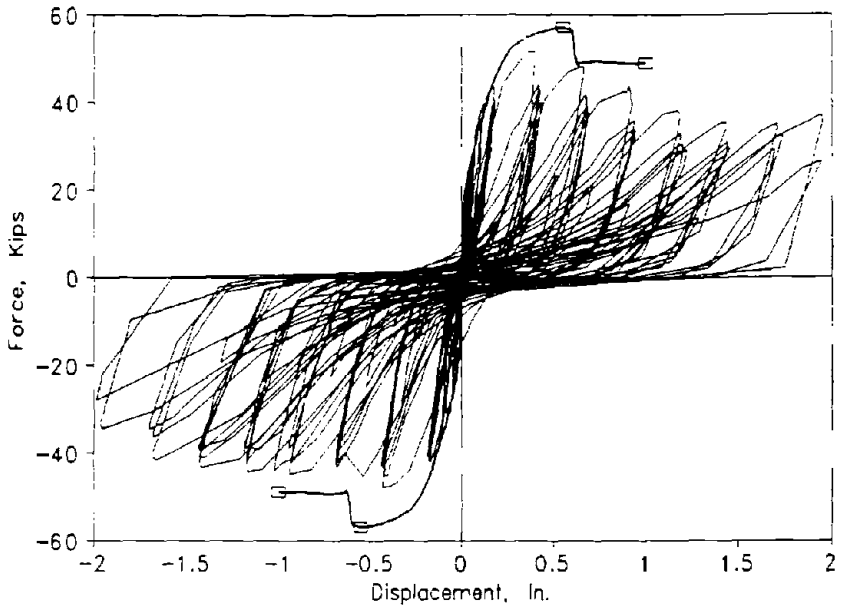

Figure 6-2. Comparison of Force-Displacement Results Between Analysis and Experiment for Wall 6.

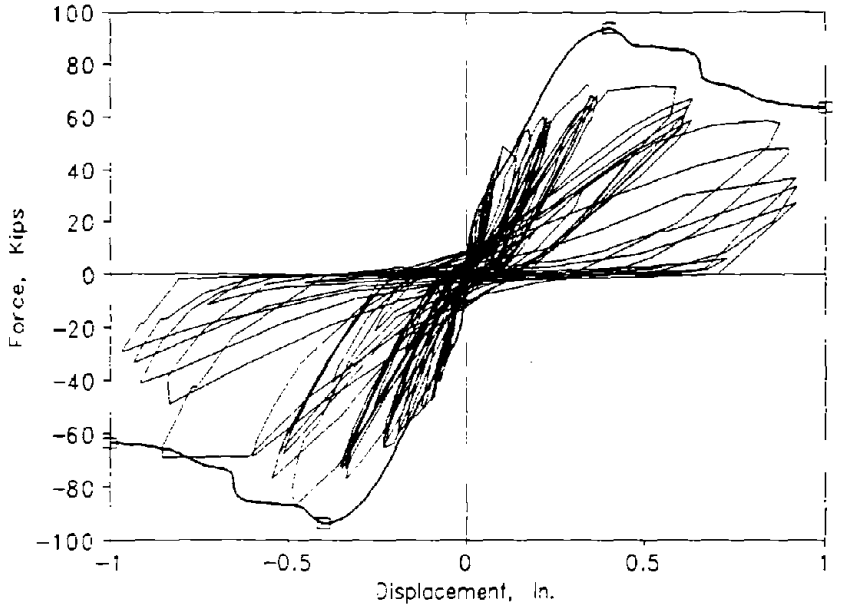

Figure 6-3. Comparison of Force-Displacement Results Between Analysis and Experiment for Wall 4.

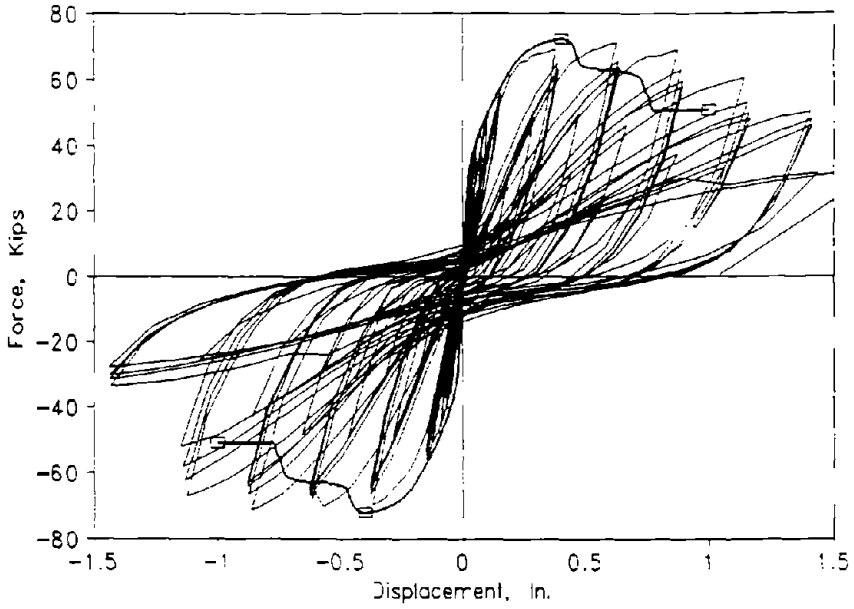

Figure 6-4. Comparison of Force-Displacement Results Between Analysis and Experiment for Wall 12.

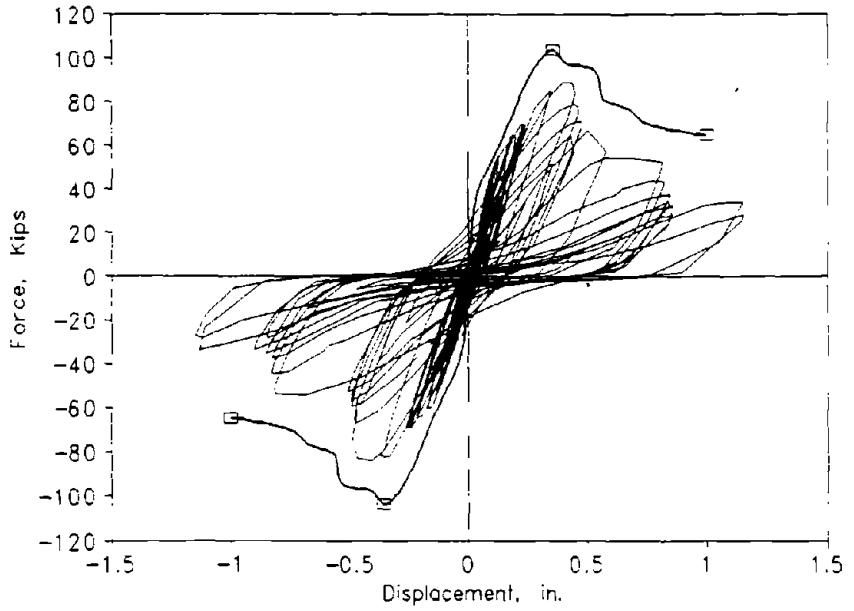

Figure 6-5. Comparison of Force-Displacement Results Between Analysis and Experiment for Wall 5.

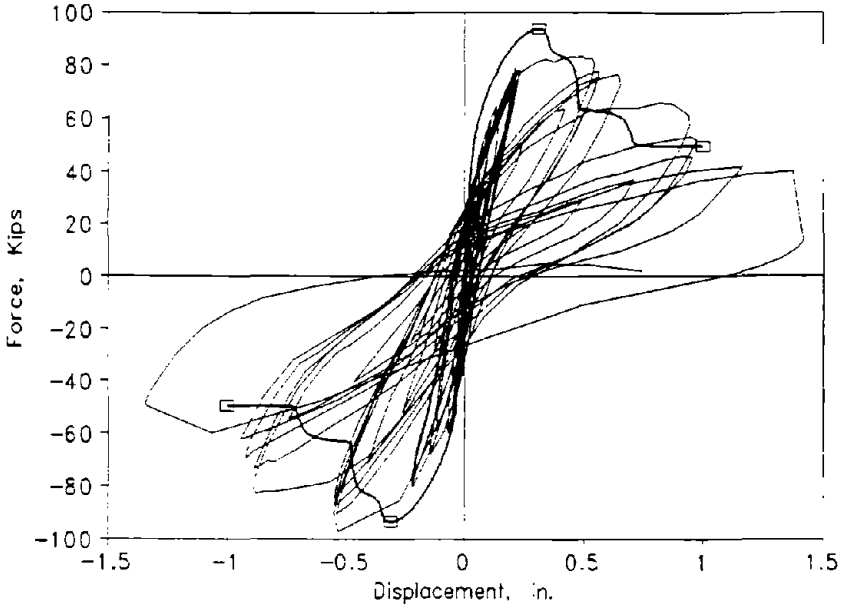

Figure 6-6. Comparison of Force-Displacement Results Between Analysis and Experiment for Wall 2.

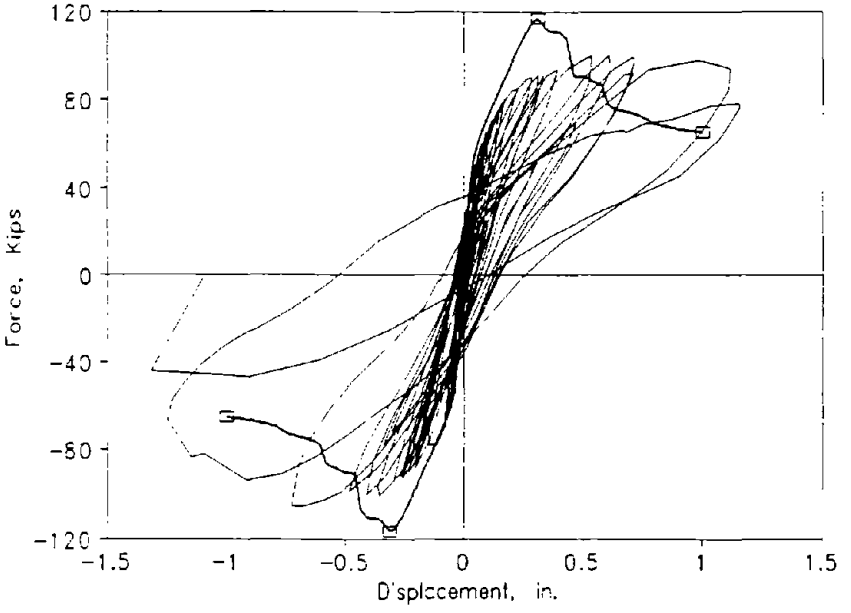

Figure 6-7. Comparison of Force-Displacement Results Between Analysis and Experiment for Wall 3.

Before the correlation between the analyses and experiments are considered, several points need to be identified.

- These calculations were performed with Version 101 of the FEM/I program [9 and 10] (the first version), which did not have many of the material refinements that are included in this revision of the User's Guide.
- Only one calculation was made for each of the walls, and no attempt was made to improve the correlation with the experiments by performing additional calculations using different material properties. Parametric studies will be conducted in the correlation phase and will be reported separately.
- We expect differences in the test results between cyclic loading and monotonic loading. In cyclic loading, differences will occur past the peak strength, since cyclic loading tends to soften the masonry on successive nonlinear cycles.
- Also, the experiments did not produce symmetrical results for the positive and negative cycles, for example Wall 3 and Wall 4 (Figures 6-7 and 6-3); and we must compare the analyses with both halves of the test results. This is most likely due to variations in the masonry materials. The experimentalist specifically noted that the masonry grout space was not completely filled in the lower (positive) corner in Wall 3 (Figure 6-7), and we expect this to be the case in some of the other specimens.

Specimens with a flexural response mode, Walls 6, 12, and 2 (Figures 6-2, 6-4, and 6-6), show tensile cracking in the masonry followed by yielding of the vertical reinforcement, softening to a peak strength, and crushing of the masonry in the compression toe. Specimens with a shear response mode, Walls 4, 5, and 3 (Figures 6-3, 6-5, and 6-7), show a major diagonal crack with the associated yielding of the horizontal reinforcement.

There is generally good agreement between peak strengths, except in Walls 5 and 6 (Figures 6-5 and 6-2), if both halves of the cyclic test results are taken into consideration. Differences in the peak values could be attributed to the variability in the uniaxial compressive strength, as indicated by the prism

strength variation (i.e., 2600 to 3200 psi). This will be investigated in future parametric studies. Also, the degradation of strength and stiffness associated with the damage factor [27] is based on reinforced concrete tests and this needs to be studied in future parametric analyses. It should be noted that unloading due to redistribution of strain during monotonic loading paths was not implemented in the version (Ver. 101) of the program that was used to conduct these calculations, and we see the possible effects of this in the analysis results. Unloading is included in the current version of the program; however, unloading for cyclic paths has not been checked out.

SECTION 7

CONCLUSIONS AND RECOMMENDATIONS

7.1 CONCLUSIONS

Although more work needs to be completed on the finite element program, the code promises to be a useful tool for the analysis of reinforced masonry building components. The results of the first correlation analyses using the current version of the FEM/I computer program with tests on reinforced masonry piers and walls are encouraging. They have shown that the code can be expected to produce good estimates of the monotonic envelope curves, as well as reproducing the sequence of events leading to the response limit states. The analytical results demonstrate that both flexural and shear type response modes can be simulated. Also, for the appropriate component configurations and loading conditions, the calculations show the capability to predict the formation of tension cracks, yielding of the vertical reinforcement, formation of vertical cracks and toe crushing, formation of diagonal cracks, and yielding of the horizontal reinforcement.

We expect the program will undergo changes and improvements as the TCCMAR program progresses. The computer program will be correlated with and validated by the experiments being conducted in the TCCMAR program. The experimental program includes tests on one-, two-, and three-story walls and a five-story building.

7.2 FUTURE RESEARCH WORK

The correlation analyses have confirmed that additional studies need to be conducted. Specific areas for further study include: the applicability of using the damage parameter, β, as defined for reinforced concrete, the influence of layup angle or joint orientation on the properties of the masonry, tension stiffening representation, effect of strain gradients on the compressive strength of masonry, and unloading for cyclic loading paths. Parametric studies are needed to identify those properties that have the most influence on the components response, and recommendations will be made for controlling the variability of these properties. Parametric studies will also be conducted to

determine the sensitivity of the FEM/I solutions to variations in the physical and material properties of the finite element model.

7.3 ACKNOWLEDGEMENT

This investigation is part of the TCCMAR Category 2 research on analytical modeling sponsored by the National Science Foundation under Grant Nos. CES-8696076, BCS-8722868, CES-8517023, and BCS-8722867. Dr. S. C. Liu is the Program Director for the National Science Foundation. He replaced Dr. A. J. Eggenberger who served as the Program Director throughout the initial phases of this research program.

Any opinions, findings, conclusions, or recommendations expressed in this paper are those of the authors and do not necessarily reflect the views of the National Science Foundation and/or the United States Government.

SECTION 8

REFERENCES

1. Agbabian Associates. "Rock Mechanics and Mining Engineering Computer Model and Code Reviews and Analysis, Vol. II: Code Implementation Topical Report" (R-8414-5650). El Segundo, CA: September 1984.

2. ASCE. *Finite Element Analysis of Reinforced Concrete*, Structural Division, Committee on Concrete and Masonry Structures. New York, N.Y.: American Society of Civil Engineers, 1982.

3. Atkinson, R.H. and Kingsley, G.R., "A Comparison of the Behavior of Clay and Concrete Masonry in Compression", Report No. 1.1-1. Atkinson-Noland & Associates, Boulder, Colorado, September 1895.

4. Bazant, Z.P., Pan, J., and Pijandier-Cabot, G., "Softening in Reinforced Concrete Beams and Frames", *Journal of Structural Engineering ASCE*, Vol. 113, No. 12, Dec. 1987.

5. Cervenca, V. "Constitutive Model for Cracked Reinforced Concrete". *Journal of the American Concrete Institute*, No. 6, Nov-Dec 1985, pp 877-882.

6. Cook, R.D. *Concepts and Applications of Finite Element Analysis.* New York, N.Y.: John Wiley and Sons, 1981.

7. Darwin, D. and Pecknold, D.A. *Inelastic Model for Cyclic Biaxial Loading of Reinforced Concrete* (SRS No. 409). Urbana-Champaign, Illinois: Civil Engineering Studies, University of Illinois, July 1974.

8. Ewing, R.D., Kariotis, J.C., Englekirk, R.E., and Hart, G.C. "Analytical Modeling For Reinforced Masonry Buildings and Components - TCCMAR Category 2 Program", *Proceedings of the Fourth North American Masonry Conference*, Los Angeles, CA, August 1987 (Vol. II) (G.C. Hart and J.C. Kariotis, Ed.). Los Angeles, CA: The Masonry Society, August 1987.

9. Ewing, R.D., El-Mustapha, A.M., and Kariotis, J.C. "A Finite Element Computer Program for the Nonlinear Static Analysis of Reinforced Masonry Walls", *8th International Brick/Block Masonry Conference*, Elsevier Applied Science Publishers, Ltd., Dublin, Ireland, September 1988.

10. Ewing, R.D., Kariotis, J.C., and El-Mustapha, A.M. "Correlation of Finite Element Analysis and Experiments on Reinforced Masonry Walls", *8th International Brick/Block Masonry Conference*, Elsevier Applied Science Publishers, Ltd., Dublin, Ireland, September 1988.

11. FEMA. *NEHRP Recommended Provisions for the Development of Seismic Regulations for New Buildings, Part I - Provisions* (Earthquake Hazards Series 17) (FEMA 95). Washington, DC: Building Seismic Safety Council (BSSC Program on Improved Seismic Safety Provisions, 1985 Edition), Federal Emergency Management Agency, February 1986.

12. Gupta, A.K. and Maestrini, S.R., "Tension-Stiffness Model for Reinforced Concrete Bars", *Journal of Structural Engineering ASCE*, Vol. 116, No. 3, March 1990, pp. 769-790.

13. Hart, G.C., Sajjad, N., Kingsley, G.R., and Noland, J.L., "Analytical Stress-Strain Curves for Grouted Concrete Masonry", *The Masonry Society Journal*, Vol. 8, No. 1, January-June, 1989, pp. T21-T34.

14. Hegemier, G.A. and Murakami, H., *Personal Communication*, Meeting at The University of California - San Diego.

15. Hinton, E. and Owen, D.R.J. *Finite Element Programming*. London, UK: Academic Press Inc. (London) Ltd., 1977.

16. Inoue, Norio, Koshika, Norihide, and Suzuki, Norio. "Analysis of Shear Wall Based on Collins Panel Test", *Proceedings of Seminar on Finite Element Analysis of Reinforced Concrete Structures*, Tokyo, Japan, May 1985 (Christian Meyer and Hajime Okamura, Ed.). New York, N.Y.: ASCE, 1985.

17. Kingsley, G.R., Atkinson, R.H., Noland, J.L., and Hart, G.C., "The Effect of Height on Stress-Strain Measurements on Grouted Concrete Masonry Prisms". *Proceedings of The 5th Canadian Masonry Symposium*, University of British Columbia, Vancouver, B.C., June 5-7, 1989.

18. Kupfer, H.B., Hilsdorf, H.K., and Rüsch, H., Behavior of Concrete Under Biaxial Stresses, *Journal of the American Concrete Institute*, Vol. 66, No. 8, Aug., 1969, pp. 656-666.

19. Maestrini, S.R. and Gupta, A.K. *Membrane Behavior of Reinforced Concrete Shell Elements Including Tension-Stiffening*. Raleigh, North Carolina: Department of Civil Engineering, North Carolina State University, February 1987.

20. Meyer, Christian and Okamura, Hajime (Ed.). "Finite Element Analysis of Reinforced Concrete Structures", Proceedings of the Seminar held in Tokyo, Japan, May 1985. New York, N.Y.: ASCE, 1985.

21. Nayak, G.C. and Zienkiewicz, O.C. "Elasto-Plastic Stress Analysis, A Generalization For Various Constitutive Relations Including Strain Softening". *International Journal of Numerical Methods in Engineering*, Vol. 5, No. 1, 1972, pp 113-135.

22. Noland, J.L. "A Review of The U. S. Coordinated Program For Masonry Building Research", *Proceedings of the Fourth North American Masonry Conference*, Los Angeles, CA, August 1987 (Vol. II) (G.C. Hart and J.C. Kariotis, Ed.). Los Angeles, CA: The Masonry Society, August 1987.

23. Owen, D.R.J. and Hinton, E. *Finite Elements In Plasticity: Theory and Practice*. Swansea, UK: Pineridge Press Limited, 1980.

24. Sajjad, N.A., "Confinement of Concrete Masonry", doctoral dissertation, University of California, Los Angeles, California, 1990.

25. Seible, Frieder and Hegemier, Gilbert. "From Materials and Components to Masonry Prototype Structures - The TCCMAR-U.S. Experimental Program", *Proceedings of the Fourth North American Masonry Conference*, Los Angeles, CA, August 1987 (Vol. II) (G.C. Hart and J.C. Kariotis, Ed.). Los Angeles, CA: The Masonry Society, August 1987.

26. Shing, P.B., Noland, J.L., Spaeh, H., and Klamerus, E. "Inelastic Behavior of Masonry Wall Panels Under In-Plane Cyclic Loads", *Proceedings of the Fourth North American Masonry Conference*, Los Angeles, CA, August 1987, (Vol. II), (G.C. Hart and J.C. Kariotis, Ed.). Los Angeles, CA: The Masonry Society, August 1987.

27. Vecchio, F.J. and Collins, M.P. *The Response of Reinforced Concrete To In-Plane Shear and Normal Stresses* (Publication No. 82-03). Toronto, Canada: University of Toronto, March 1982.

28. Yankelevsky, D.Z. and Reinhardt, H.W. "Model for Cyclic Compressive Behavior of Concrete". *Journal of Structural Engineering ASCE*, Vol. 113, No. 2, February 1987, pp. 228-240.

29. Zienkiewicz, O.C. *The Finite Element Method, 3rd Edition*. New York, N.Y.: McGraw-Hill Book Co., 1977.

30. Zienkiewicz, O.C., Valliappan, S. and King, I.P. "Elasto-Plastic Solutions of Engineering Problems; Initial Stress Finite Element Approach". *International Journal of Numerical Methods in Engineering*, Vol. 1, 1969, pp 75-100.

APPENDIX A

DEMONSTRATION ANALYSIS MODEL

Introduction - The following analysis model is intended to demonstrate the use of the FEM/I computer program and to serve as a guide for the preparation of the input data for a typical application. The analysis model was selected from those used in parametric studies that are being conducted to determine the sensitivity of the FEM/I solutions to variations in the physical and material properties of the finite element model.

Demonstration Analysis Description - The model simulates the static testing of a cantilever reinforced masonry wall subjected to a constant vertical axial load and a monotonic horizontal displacement loading applied at its top. The masonry wall is 72 in. wide, 120 in. high, and 5 5/8 in. thick fabricated with 6 x 8 x 16 in. hollow concrete block units (i.e., 4 1/2 units wide, 15 courses high, and 1 unit thick) and is fully grouted. The vertical reinforcement is comprised of 5 #6 bars spaced 16 in. apart. The horizontal reinforcement is comprised of 8 #4 bars; the lower 7 bars are spaced 16 in. apart and the 8^{th} bar is 8 in. above the 7^{th} bar. The wall is fabricated on a reinforced concrete base 120 in. wide, 18 in. high, and 18 in. thick. The vertical reinforcement in the wall is continued into and secured in the base.

Finite Element Model - The finite element mesh used in the analysis is shown in Figure A-1 and it is drawn with a scale of 1 in. to 20 in. The model has 80 elements and 103 nodal points. The concrete base is represented by elements 1 through 20 and the masonry wall is represented by elements 21 through 80. The origin of the coordinate system is at nodal point 28 (shown with a circle enclosing an X), where the x-coordinate is positive to the right and the y-coordinate is positive upwards. The concrete base is pinned at its lowest level at nodal points 1 through 11 (shown with triangles). The vertical axial load of 20 psi is applied downward along the top edge of the wall at elements 75 through 80. The monotonic horizontal displacement is applied at the top of the wall at nodal points 98, 100, and 102 (shown with a circle).

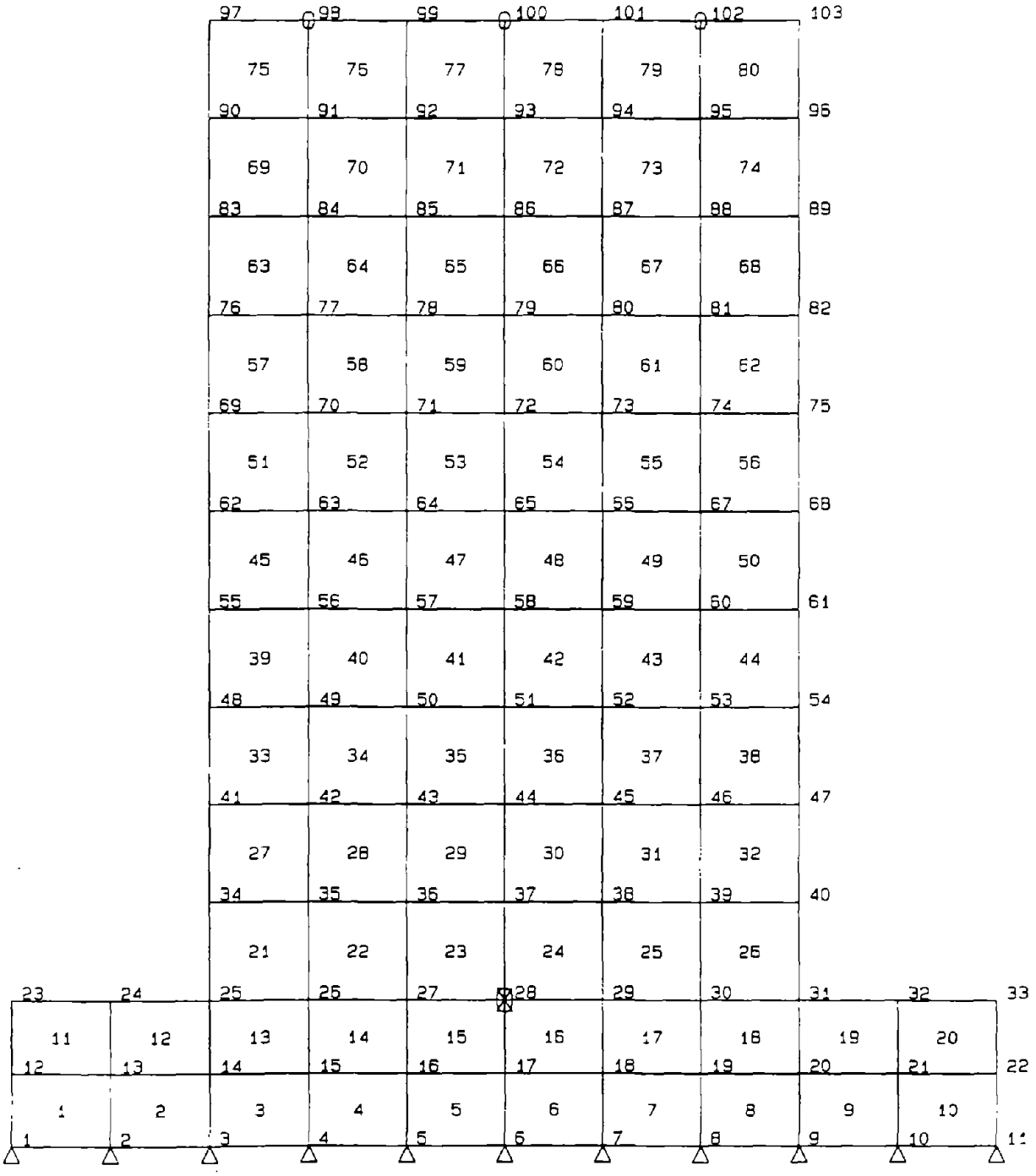

Figure A-1. Finite Element Mesh For Demonstration Analysis Model. (Scale 1 in. = 20 in.)

Material Properties - The material properties used for the analysis are given below:

Reinforced Masonry Wall	Reinforced Concrete Base
ν = 0.16	ν = 0.20
f_m = 3000 psi	f_m = 4500 psi ($f_m = f'_c$)
ϵ_o = 0.0022	ϵ_o = 0.003
A_1 = 2	A_1 = 2
A_2 = 2	A_2 = 2
A_3 = 0.1	A_3 = 0.1
A_4 = 0.6	A_4 = 0.6
MCD = 2 (β = 1.0)	MCD = 2 (β = 1.0)
f_{cr} = 100 psi	f_{cr} = 475 psi ($f_{cr} = 7.1\sqrt{f'_c}$)
E_t = 3 x 10^6 psi	E_t = 3.8 x 10^6 psi ($E_t = 57\sqrt{f'_c}$)
MTS = 2 (TS Model No. 2)	MTS = 2 (TS Model No. 2)
B_1 = 0.5	B_1 = 0.5
α = 0.18	α = 0.25
E_s = 29 x 10^6 psi	E_s = 29 x 10^6 psi
ζ = 2%	ζ = 2%
$\rho_v = \frac{5 \times 0.44}{72 \times 5\ 5/8} = 0.0054$	ρ_v = 0.007
$\rho_h = \frac{7 \times 0.196}{(120-8) \times 5\ 5/8} = 0.0022$	ρ_h = 0.007
f_{yv} = 65,000 psi	f_{yv} = 65,000 psi
f_{yh} = 65,000 psi	f_{yh} = 65,000 psi

Reinforced Masonry Wall, Top Row of Elements

The material properties are similar to those given above, except for the additional horizontal reinforcement.

$\rho_h = 2 \times 0.0022 = 0.0044$

The Tension Stiffening Parameters

Suggested values for the tension stiffening parameters α and B_1 are given in Table A-2 for several values of ρ.

Input Data File - The input data file for this analysis model is given in Table A-1. The preparation of the input data follows directly from the model description and material property data given above and the instructions given in Section 5. However, for clarity additional comments are given below for some of the data entries.

Card Group 3

NVFIX = 14 Eleven (11) nodes have pinned boundary conditions and 3 nodes have prescribed displacement.

NNODE = 4 The nonlinear element has only 4 nodes.
Linear elements can have 4, 8, or 9 nodes.

NMATS = 3 1 - Reinforced Concrete Base.
2 - Reinforced Masonry Wall, main body of the wall.
3 - Reinforced Masonry Wall, top course has additional horizontal reinforcement.

Card Group 4

Elements 1 to 20 have material property 1.
Elements 21 to 74 have material property 2.
Elements 75 to 80 have material property 3.
Specifying the element nodal connectivity numbers by starting at the same corner of each element (lower left hand corner in this case) guarantees that the Gauss points of all of the elements will be located in the same relative position. This is invaluable in the interpretation of the element stresses and strains.

Card Group 6

Nodal points 98, 100, and 102 have prescribed displacements in the x-direction and are free to translate in the y-direction. Therefore, the constraint code IFPRE is 10. Although any value could be used, the value of the x-component of the prescribed displacement PRESC(1) has been arbitrarily set to 1.0 so that the values given for FACTD in Card Group 18 are the actual displacements to be attained in the given load step.

Card Group 8

Not required - no initial stress.

Card Group 9

NUMFDF = 3 To facilitate the interpretation of the output, the sum of the reactions at 3 nodal points (NODE1 = 100, NODE2 = 98, and NODE3 = 102, i.e., the nodes with prescribed displacement) will be directed to the Force-Deflection file along with the prescribed displacement at 1 nodal point (NODE1 = 100).

KOMPNT = 1 The x-component of the 3 reactions and the 1 displacement are to be output to the Force-Deflection file.

Card Group 14

Not required - no nodal point loading.

Card Group 15

Not required - no gravity loading.

Card Group 16

NEDGE = 6 Vertical axial pressure load is applied to the top edge of elements 75 through 80.

Card Group 17

NOPRS(1) and NOPRS(2)

Specify the nodal points for each loaded element in a counterclockwise sequence.

PRES(1,1) and PRES(2,1)

The normal load on an element is specified as a force per unit length (20 psi x 5 5/8 in. thickness = 0.1125 kips per in.). A positive value indicates that the load acts downward (i.e., into the element).

Card Group 18

The load increment controls will generate 33 load/displacement increments. The convergence tolerance TOLER and maximum number of iterations MITER are set to 5% and 50, respectively, for all increments.

The first card (FACTE = 1.0, FACTD = 0.0, and NDIV = 1) will generate 1 increment where all of the vertical axial load is applied in the 1st increment (FACTE = 1.0) before any horizontal prescribed displacements are applied (FACTD = 0.0). In the remaining increments the vertical axial load is held constant (FACTE = 1.0) and the horizontal prescribed displacements are applied in increments of 0.025 in. (initial increments) and 0.05 in. (remaining increments).

The second card (FACTD = 0.1 and NDIV = 4) will generate 4 increments to move from the previous displacement of 0.0 in. to 0.1 in.
dx = 0.1/4 = 0.025 in.

The third card (FACTD = 0.2 and NDIV = 2) will generate 2 increments to move from the previous displacement of 0.1 in. to 0.2 in.
dx = (0.2-0.1)/2 = 0.05 in.

The remaining cards generate increments in a similar manner. The load increment control data is terminated when NDIV = -1.

Sample Output - Figure A-2 shows the force-displacement (i.e., base shear-top displacement) envelope for the reinforced masonry wall of the demonstration analysis model. The peak strength of 46.1 kips is reached at a horizontal displacement of 0.80 in. (indicated by the square symbol). The figure shows that toe crushing occurs just after the peak strength is reached.

Table A-1. FEM/I Input Data For Demonstration Analysis.

Card Group	Input Data
1	START
2	Parametric Study - PS1-17.Inp, Mesh 1, Nominal Properties, dx = 0.05", in -kip
3	103 80 14 1 4 3 0 0 0
4	1 1 1 2 13 12
	2 1 2 3 14 13
	3 1 3 4 15 14
	4 1 4 5 16 15
	5 1 5 6 17 16
	6 1 6 7 18 17
	7 1 7 8 19 18
	8 1 8 9 20 19
	9 1 9 10 21 20
	10 1 10 11 22 21
	11 1 12 13 24 23
	12 1 13 14 25 24
	13 1 14 15 26 25
	14 1 15 16 27 26
	15 1 16 17 28 27
	16 1 17 18 29 28
	17 1 18 19 30 29
	18 1 19 20 31 30
	19 1 20 21 32 31
	20 1 21 22 33 32
	21 2 25 26 35 34
	22 2 26 27 36 35
	23 2 27 28 37 36
	24 2 28 29 38 37
	25 2 29 30 39 38
	26 2 30 31 40 39
	27 2 34 35 42 41
	28 2 35 36 43 42
	29 2 36 37 44 43
	30 2 37 38 45 44
	31 2 38 39 46 45
	32 2 39 40 47 46
	33 2 41 42 49 48
	34 2 42 43 50 49
	35 2 43 44 51 50
	36 2 44 45 52 51
	37 2 45 46 53 52
	38 2 46 47 54 53
	39 2 48 49 56 55
	40 2 49 50 57 56
	41 2 50 51 58 57
	42 2 51 52 59 58
	43 2 52 53 60 59
	44 2 53 54 61 60
	45 2 55 56 63 62
	46 2 56 57 64 63
	47 2 57 58 65 64
	48 2 58 59 66 65
	49 2 59 60 67 66
	50 2 60 61 68 67
	51 2 62 63 70 69
	52 2 63 64 71 70
	53 2 64 65 72 71
	54 2 65 66 73 72
	55 2 66 67 74 73
	56 2 67 68 75 74
	57 2 69 70 77 76
	58 2 70 71 78 77
	59 2 71 72 79 78 . . . . . more

Table A-1. FEM/I Input Data For Demonstration Analysis. (Continued)

Card Group	Input Data
4	60 2 72 73 80 79
	61 2 73 74 81 80
	62 2 74 75 82 81
	63 2 76 77 84 83
	64 2 77 78 85 84
	65 2 78 79 86 85
	66 2 79 80 87 86
	67 2 80 81 88 87
	68 2 81 82 89 88
	69 2 83 84 91 90
	70 2 84 85 92 91
	71 2 85 86 93 92
	72 2 86 87 94 93
	73 2 87 88 95 94
	74 2 88 89 96 95
	75 3 90 91 98 97
	76 3 91 92 99 98
	77 3 92 93 100 99
	78 3 93 94 101 100
	79 3 94 95 102 101
	80 3 95 96 103 102
5	1 -60.00 -18.00
	2 -48.00 -18.00
	3 -36.00 -18.00
	4 -24.00 -18.00
	5 -12.00 -18.00
	6 0.00 -18.00
	7 12.00 -18.00
	8 24.00 -18.00
	9 36.00 -18.00
	10 48.00 -18.00
	11 60.00 -18.00
	12 -60.00 -9.00
	13 -48.00 -9.00
	14 -36.00 -9.00
	15 -24.00 -9.00
	16 -12.00 -9.00
	17 0.00 -9.00
	18 12.00 -9.00
	19 24.00 -9.00
	20 36.00 -9.00
	21 48.00 -9.00
	22 60.00 -9.00
	23 -60.00 0.00
	24 -48.00 0.00
	25 -36.00 0.00
	26 -24.00 0.00
	27 -12.00 0.00
	28 0.00 0.00
	29 12.00 0.00
	30 24.00 0.00
	31 36.00 0.00
	32 48.00 0.00
	33 60.00 0.00
	34 -36.00 12.00
	35 -24.00 12.00
	36 -12.00 12.00
	37 0.00 12.00
	38 12.00 12.00
	39 24.00 12.00
	40 36.00 12.00
	41 -36.00 24.00 . . . . . more

Table A-1. FEM/I Input Data For Demonstration Analysis. (Continued)

Card Group	Input Data			
5	42	-24.00	24.00	
	43	-12.00	24.00	
	44	0.00	24.00	
	45	12.00	24.00	
	46	24.00	24.00	
	47	36.00	24.00	
	48	-36.00	36.00	
	49	-24.00	36.00	
	50	-12.00	36.00	
	51	0.00	36.00	
	52	12.00	36.00	
	53	24.00	36.00	
	54	36.00	36.00	
	55	-36.00	48.00	
	56	-24.00	48.00	
	57	-12.00	48.00	
	58	0.00	48.00	
	59	12.00	48.00	
	60	24.00	48.00	
	61	36.00	48.00	
	62	-36.00	60.00	
	63	-24.00	60.00	
	64	-12.00	60.00	
	65	0.00	60.00	
	66	12.00	60.00	
	67	24.00	60.00	
	68	36.00	60.00	
	69	-36.00	72.00	
	70	-24.00	72.00	
	71	-12.00	72.00	
	72	0.00	72.00	
	73	12.00	72.00	
	74	24.00	72.00	
	75	36.00	72.00	
	76	-36.00	84.00	
	77	-24.00	84.00	
	78	-12.00	84.00	
	79	0.00	84.00	
	80	12.00	84.00	
	81	24.00	84.00	
	82	36.00	84.00	
	83	-36.00	96.00	
	84	-24.00	96.00	
	85	-12.00	96.00	
	86	0.00	96.00	
	87	12.00	96.00	
	88	24.00	96.00	
	89	36.00	96.00	
	90	-36.00	108.00	
	91	-24.00	108.00	
	92	-12.00	108.00	
	93	0.00	108.00	
	94	12.00	108.00	
	95	24.00	108.00	
	96	36.00	108.00	
	97	-36.00	120.00	
	98	-24.00	120.00	
	99	-12.00	120.00	
	100	0.00	120.00	
	101	12.00	120.00	
	102	24.00	120.00	
	103	36.00	120.00	. . . . . more

Table A-1. FEM/I Input Data For Demonstration Analysis. (Continued)

Card Group	Input Data
6	1 11 0.00 0.00 2 11 0.00 0.00 3 11 0.00 0.00 4 11 0.00 0.00 5 11 0.00 0.00 6 11 0.00 0.00 7 11 0.00 0.00 8 11 0.00 0.00 9 11 0.00 0.00 10 11 0.00 0.00 11 11 0.00 0.00 98 10 1.00 0.00 100 10 1.00 0.00 102 10 1.00 0.00
7	1 'Reinforced Concrete Base' 0.20 18.0 0.0 1 4.5 0.003 2.0 2.0 0.1 0.6 2 0.475 3800.0 2 0.5 0.25 29000.0 0.02 0.007 0.007 65.0 65.0 2 'Reinforced Masonry Wall' 0.16 5.625 0.0 1 3.0 0.0022 2.0 2.0 0.1 0.6 2 0.100 3000.0 2 0.5 0.18 29000.0 0.02 0.0054 0.0022 65.0 65.0 3 'Reinforced Masonry Wall, Top Course' 0.16 5.625 0.0 1 3.0 0.0022 2.0 2.0 0.1 0.6 2 0.100 3000.0 2 0.5 0.18 29000.0 0.02 0.0054 0.0044 65.0 65.0
9	60 77 3 1 100 98 102
10	21 22 23 24 25 26 27 28 29 30 31 32 33 34 35 36 37 38 39 40 41 42 43 44 45 46 47 48 49 50 51 52 53 54 55 56 57 58 59 60 61 62 63 64 65 66 67 68 69 70 71 72 73 74 75 76 77 78 79 80
11	25 26 27 28 29 30 31 34 35 36 37 38 39 40 41 42 43 44 45 46 47 48 49 50 51 52 53 54 55 56 57 58 59 50 61 62 63 64 65 66 67 68 69 70 71 72 73 74 75 76 77 78 79 80 81 82 83 84 85 86 87 88 89 90 91 92 93 94 95 96 97 98 99 100 101 102 103 . . . . . more

Table A-1. FEM/I Input Data For Demonstration Analysis. (Concluded)

Card Group	Input Data
12	Parametric Study - PS1-17.Inp, Mesh 1, Nominal Properties, dx = 0.05", in.-kip
13	0 0 1
16	6
17	75 98 97 0.1125 0.00 0.1125 0.00 76 99 98 0.1125 0.00 0.1125 0.00 77 100 99 0.1125 0.00 0.1125 0.00 78 101 100 0.1125 0.00 0.1125 0.00 79 102 101 0.1125 0.00 0.1125 0.00 80 103 102 0.1125 0.00 0.1125 0.00
18	1 0.0 0.0 1.0 0.0 5.0 50 3 1 0 0 4 0.0 0.0 1.0 0.1 5.0 50 3 1 0 0 2 0.0 0.0 1.0 0.2 5.0 50 3 1 0 0 2 0.0 0.0 1.0 0.3 5.0 50 3 1 0 0 2 0.0 0.0 1.0 0.4 5.0 50 3 1 0 0 2 0.0 0.0 1.0 0.5 5.0 50 3 1 0 0 2 0.0 0.0 1.0 0.6 5.0 50 3 1 0 0 2 0.0 0.0 1.0 0.7 5.0 50 3 1 0 0 2 0.0 0.0 1.0 0.8 5.0 50 3 1 0 0 2 0.0 0.0 1.0 0.9 5.0 50 3 1 0 0 2 0.0 0.0 1.0 1.0 5.0 50 3 1 0 0 2 0.0 0.0 1.0 1.1 5.0 50 3 1 0 0 2 0.0 0.0 1.0 1.2 5.0 50 3 1 0 0 2 0.0 0.0 1.0 1.3 5.0 50 3 1 0 0 2 0.0 0.0 1.0 1.4 5.0 50 3 1 0 0 2 0.0 0.0 1.0 1.5 5.0 50 3 1 0 0 -1 0.0 0.0 0.0 0.0 0.0 0 0 0 0 0

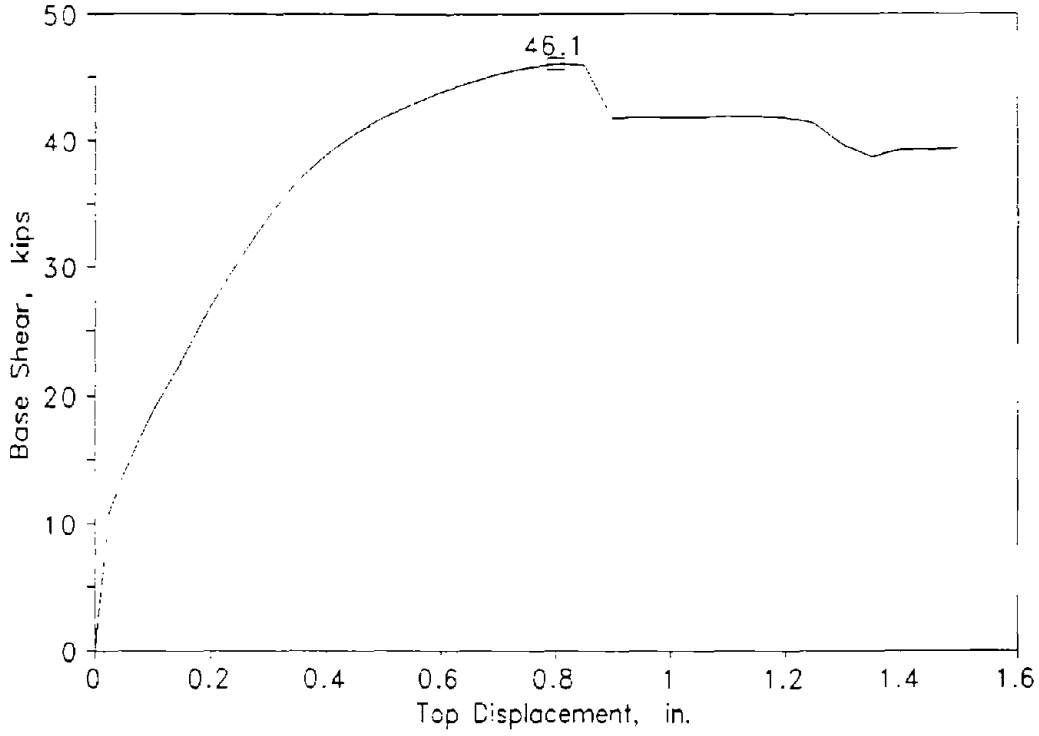

Figure A-2. Force-Displacement Envelope For Demonstration Analysis Model.

Table A-2. Suggested Values for Tension Stiffening Parameters.

ρ	α	B_1
0.0025	0.06	0.38
0.0035	0.10	0.48
0.0050	0.18	0.5
0.0075	0.25	0.5

APPENDIX B

FEM-CALC PROCESSOR
PROGRAMMING DOCUMENTATION

This appendix provides some basic documentation for the main calculation and solution processor. The documentation includes

- A program structure diagram.
- A description of the program subroutines.
- A description of each variable in the program labeled common blocks.
- A description of the files used by the program.
- A description of the material properties array.
- A description of the major event file array.

This documentation is not intended to be complete, and is provided only as an aid to the user who may wish to modify the program.

FEM-CALC PROGRAM STRUCTURE

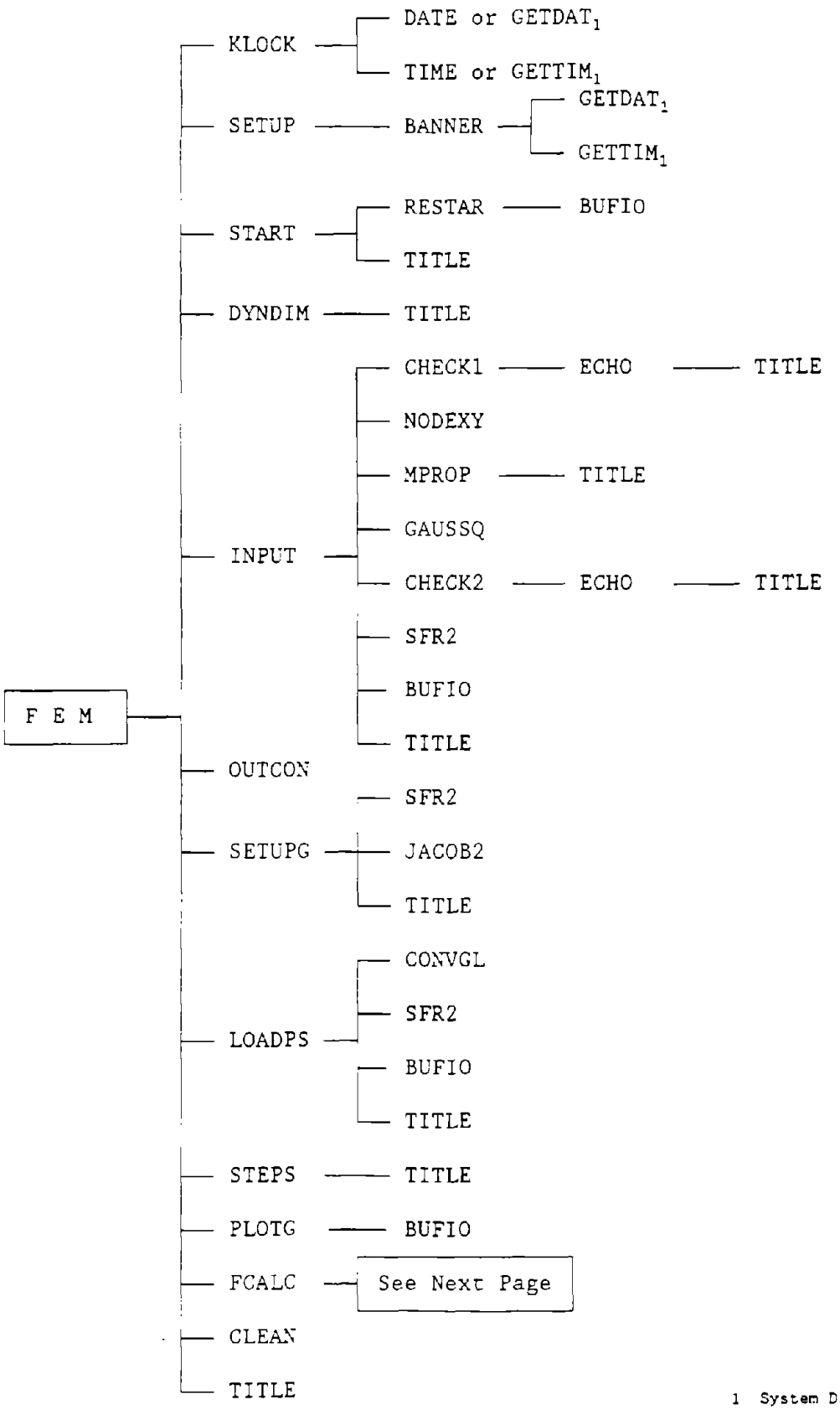

1 System Date and Time routines.

FEM-CALC PROGRAM STRUCTURE (Concluded)

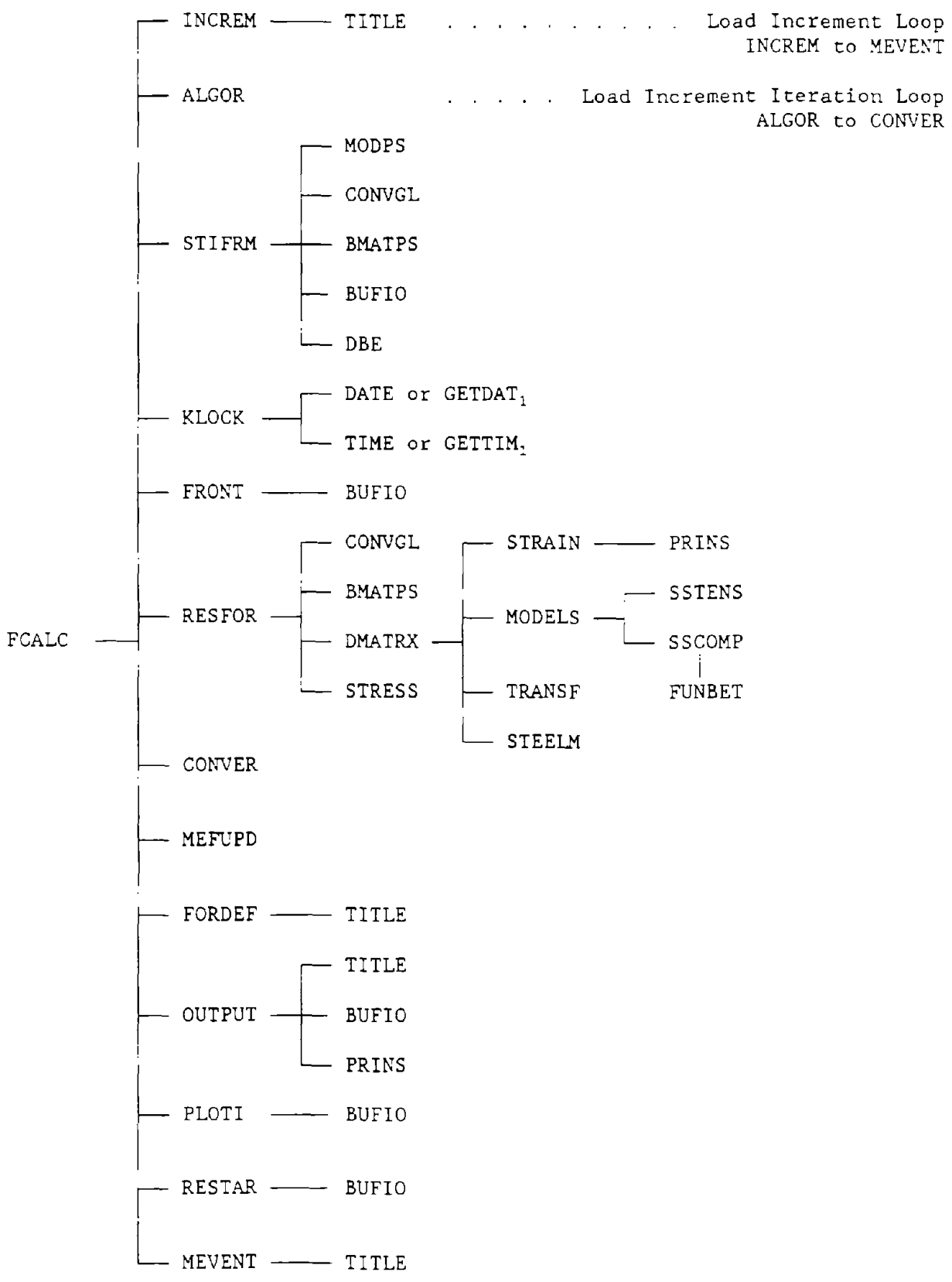

1 System Date and Time routines.

FEM-CALC PROGRAM SUBROUTINES

Subroutine		Description
FEM	-	Main driver for FEM/I. Controls the program initialization, setup, reading of the input data, dynamic allocation, and calculations.
ALGOR	-	Sets the equation resolution index, KRESL.
BANNER	-	Print the program banner page.
BMATPS	-	Evaluate the strain-displacement matrix, B.
BUFIO	-	Binary input/output of arrays using a maximum buffer size.
CHECK1	-	Check main control variables.
CHECK2	-	Check discretization data and nodal destination data required by subroutine FRONT.
CLEAN	-	Perform program wrap up tasks.
CONVER	-	Determines when the solution has converged.
CONVGL	-	Convert the global arrays calculated in SETUPG into local arrays for a single Gauss point.
DBE	-	Multiply two matrices, D x B.
DMATRX	-	Evaluate the secant material matrices for each Gauss point of all elements.
DYNDIM	-	Perform dynamic allocation / dimensioning.
ECHO	-	Read and write remaining data cards if an error was detected in subroutines CHECK1 or CHECK2.
FCALC	-	Main control driver for the calculations.
FORDEF	-	Output the force and displacement at a selected node.
FRONT	-	Equation solver for a system of algebraic equations using the frontal solution method.
FUNBET	-	Evaluate the damage factor, β.
GAUSSQ	-	Set Gaussian quadrature constants.
INCREM	-	Increment the prescribed displacement and applied loading.
INPUT	-	Read and print most of the input data.
INVERT	-	Invert a third or fourth order matrix.
JACOB2	-	Compute the global coordinates of a Gauss point, the Jacobian matrix, and the derivatives of the shape functions with respect to the global coordinates.
KLOCK	-	Time in seconds since last call.
LOADPS	-	Evaluate the consistent nodal forces for each element due to surface tractions, gravity forces, or point loads.
MEFUPD	-	Update the major event file data at the end of each load step after solution convergence.
MEVENT	-	Output a record of the major events for each element (i.e., masonry cracking, peak strength, and crushing and yielding of the horizontal and vertical reinforcement).
MODELS	-	Controls the calculation of the secant material moduli.
MODPS	-	Evaluate the elasticity matrix, D, for a plane stress, plane strain, or axisymmetric problem.
MPROP	-	Read and print material property data.

FEM-CALC PROGRAM SUBROUTINES (Continued)

Subroutine		Description
NODEXY	-	Interpolate for the midside nodes of eight-noded elements and the central node of nine-noded isoparametric elements.
OUTCON	-	Read output control variables.
OUTPUT	-	Output displacements, stresses, strains, and reactions.
PLOTG	-	Output nodal point coordinates and element connectivity to the postprocessing file.
PLOTI	-	Output response quantities to postprocessing file.
PRINS	-	Evaluate the principal strains and stresses.
RESFOR	-	Controls the numerical integration for all elements. Evaluate the total strain and stress, and calculate the residual force vector.
RESTAR	-	Read or write restart files.
SETUP	-	Perform initial program setup tasks. Preset labeled common blocks, and open input and output files.
SETUPG	-	Compute shape function values and global derivatives, radial coordinates, and integration weighting factors for all Gauss points within the finite element mesh. Store this data in arrays.
SFR2	-	Evaluate shape functions and their derivatives with respect to the local isoparametric coordinates.
SSCOMP	-	Evaluate the secant modulus in the orthotropic directions for compressive principal strains.
SSTENS	-	Evaluate the secant modulus in the orthotropic directions for tensile principal strains.
START	-	Read program execution option and control parameters. Open program files.
STEELM	-	Evaluate the material matrices for the reinforcement.
STEPS	-	Generate a step-by-step load increment control file.
STIFRM	-	Evaluate the stiffness matrix for each element.
STRAIN	-	Evaluate the total, incremental, and total principal strains at all Gauss points.
STRESS	-	Evaluate total and incremental strain and stress at all Gauss points.
TITLE	-	Print top of output page with logo, program version number, problem title, and page number.
TRANSF	-	Evaluate the secant material matrices for the masonry in the orthotropic directions and transform the material matrices into the global coordinate system.

FEM-CALC PROGRAM LABELED COMMON BLOCKS

Program Units and Page Controls

```
COMMON /IUNITS/ KONS, IN, IO, LINES, NPAGE, MAXLIN, MBYTE
```

KONS	=	Logical unit no. of the console, 0.
IN	=	Logical unit no. for the input file, 5.
IO	=	Logical unit no. for the output file, 6.
LINES	=	Line counter.
NPAGE	=	Page counter.
MAXLIN	=	Maximum no. of data lines per page, does not include logo, page counter, or data title information, 50.
MBYTE	=	Binary I/O buffer size in bytes, 4000.

Program File Names

```
COMMON /FNAMES/ FNAME1, FNAME2, FNAME3, FNAME4, FNAME5, FNAME6
```

FNAME1	=	File name of the input data file.
FNAME2	=	File name of the output data file.
FNAME3	=	File name of the postprocessing data file.
FNAME4	=	File name of the force-deflection file.
FNAME5	=	File Name of the major event file.
FNAME6	=	File Name of the restart file.

All file names are 12 characters in length.

Program and Problem Titles

```
COMMON /TITLES/ LOGO(20), JOBHED(20)
```

LOGO	=	Program name and revision number (80 characters, 4 characters per word). Printed at the top of each new page of output.
JOBHED	=	Problem title (80 Characters, 4 characters per word). Printed at the top of each new page of output.

Program Constants

```
COMMON /CONSTS/ BLANK, RADIAN, PIE, GRAV
```

BLANK	=	Four blank characters.
RADIAN	=	Pi / 180.0.
PIE	=	Pi = 3.141592.....
GRAV	=	386.0, Acceleration of gravity in in./sec.^{2}

Problem Control Parameters

COMMON /KONTRL/ NNN(40)

NNN(1),	NPOIN	= No. of nodal points.
NNN(2),	NELEM	= No. of elements.
NNN(3),	NVFIX	= No. of constrained nodal points.
NNN(4),	NTYPE	= Parameter defining the problem type (1, 2, or 3).
NNN(5),	NNODE	= No. of nodes per element (4, 8, or 9).
NNN(6),	NMATS	= No. of different materials.
NNN(7),	NGAUS	= Order of the numerical integration formula used for the elements (2 or 3).
NNN(8),	NEVAB	= NNODE*NDOFN = 2*NNODE .
NNN(9),	NALGO	= Parameter defining the solution algorithm.
NNN(10),	NRSTR	= No. of rows in the strain array, STRPL, 20.
NNN(11),	NINCS	= No. of increments in which the loading is applied.
NNN(12),	IPFLAG	= Postprocessor file generation flag.
NNN(13),	NSTR1	= Maximum no. of stress components per Gauss/nodal pt. (4).
NNN(14),	NTOTV	= NPOIN*NDOFN = 2*NPOIN .
NNN(15),	NGAU2	= NGAUS*NGAUS .
NNN(16),	NTOTG	= NELEM*NGAU2 .
NNN(17),	MBUFA	= No. of equations in calculation buffer.
NNN(18),	MELEM	= . . . . . Available
NNN(19),	MEVAB	= MBYTE, Binary I/O buffer size in bytes, 4000.
NNN(20),	MFRON	= Frontalwidth.
NNN(21),	MMATS	= . . . . . Available
NNN(22),	MPOIN	= . . . . . Available
NNN(23),	MSTIF	= Maximum length required for the global stiffness array. (MFRON*MFRON-MFRON)/2 + MFRON .
NNN(24),	MTOTG	= IOFLG, a flag that allows splitting of large output files, 0 =, no splitting; 1 =, split output file.
NNN(25),	MTOTV	= NPRINT, file counter for IOFLG above.
NNN(26),	MVFIX	= LDFLG, encoded load control flag.
NNN(27),	NDOFN	= No. of degrees-of-freedom per node (2).
NNN(28),	NPROP	= No. of physical properties for each material (35).
NNN(29),	NSTRE	= No. of stress components per point (3 or 4).
NNN(30),	IREST	= Restart flag.
NNN(31),	MTOGN	= NTOTG*NNODE = NGAU2*NNODE*NELEM .
NNN(32),	IINCS	= No. of load increments completed.
NNN(33),	ITEMP	= No. of characters in input data file name, FNAME1.
NNN(34),	INISR	= Initial stress flag.
NNN(35),	INITP	= . . . . . Available
NNN(36),	ISTAR	= Restart file generation flag.
NNN(37),	NSTEP	= No. of load increments generated and stored on File 8.
NNN(38),	NBLOK	= No. of blocks used to store the global stiffness matrix.
NNN(39),	NCYCL	= No. of load step/iteration cycles completed.
NNN(40),	IELAS	= Elastic analysis flag.

Blank Common Addresses

```
COMMON /ADDRES/ NR1, ..., NR33, NRVAR,
                NI1, ..., NI15, NIVAR
```

NR1	= ASDIS(NTOTV)	=	Incremental nodal displacements.
NR2	= COORD(NPOIN,2)	=	Nodal point x and y (or r and z) coordinates.
NR3	= ELOAD(NELEM,NEVAB)	=	Incremental nodal loads.
NR4	= ESTIF(NEVAB,NEVAB)	=	Element stiffness matrix.
NR5	= GDVOL(NTOTG)	=	Integration weightings at all Gauss points.
NR6	= GRADG(NTOTG)	=	Radial coordinates at all Gauss points.
NR7	= FIXED(NTOTV)	=	Incremental prescribed nodal displacements.
NR8	= POSGP(4)	=	Local coordinates for a Gauss point (Gauss-Legendre integration constants).
NR9	= GLYDS(MTOGN)	=	Shape function global derivatives at all Gauss points, y or z direction.
NR10	= GLSHP(MTOGN)	=	Shape function global values at all Gauss points.
NR11	= GLXDS(MTOGN)	=	Shape function global derivatives at all Gauss points, x or r direction.
NR12	= PRESC(NVFIX,NDOFN)	=	Prescribed x and y (or r and z) displacements at constrained nodes.
NR13	= EQRHS(MBUFA)	=	Reduced right hand side load terms used in equation solution.
NR14	= GLOAD(MFRON)	=	Global load vector used in equation solution.
NR15	= EQUAT(MFRON,MBUFA)	=	Reduced frontal equations used in equation solution.
NR16	=	=	. . . . . Available
NR17	= PROPS(NMATS,NPROP)	=	Material properties.
NR18	= RLOAD(NELEM,NEVAB)	=	Equivalent total nodal loads.
NR19	=	=	. . . . . Available
NR20	= STRGC(4,NTOTG)	=	Masonry total stresses at all Gauss points.
NR21	= STRG(4,NTOTG)	=	Element total stresses (Masonry and the reinforcement combined based on gross area) at all Gauss points.
NR21	= GPXYC(2,NTOTG)	=	Gauss point coordinates for postprocessor (temporary SETUPG to PLOTG).
NR22	= STRSGI(4,NTOTG)	=	Initial total stresses at all Gauss points.
NR23	= TOFOR(NTOTV)	=	Total external force vector.
NR24	= TREAC(NVFIX,2)	=	Reactions at the constrained nodes.
NR25	= TDISP(NTOTV)	=	Total nodal displacements.

Blank Common Addresses (continued)

```
COMMON /ADDRES/ NR1, ..., NR33, NRVAR,
                NI1, ..., NI15, NIVAR
```

NR26	= STFOR(NTOTV)	=	Residual force vector.
NR27	= TLOAD(NELEM,NEVAB)	=	Total nodal loads.
NR28	= STRPL(20,NTOTG)	=	Principal and global total strain data at all Gauss points.
NR29	= WEIGP(4)	=	Gauss-Legendre integration constants at a Gauss point.
NR30	=	=	. . . . . Available
NR31	= STRGS(4,NTOTG)	=	Steel total stresses at all Gauss points (gross area).
NR32	= VECRV(MFRON)	=	Calculated displacements used in equation solution.
NR33	= GSTIF(MSTIF)	=	Global stiffness matrix used in equation solution.

NRTOT = Length of blank common real array for dynamic allocation of problem dependent real arrays.

NI1	= IFFIX(NTOTV)	=	Degree-of-freedom restraint code (= 0, free; = 1, restrained).
NI2	= MEFIL(NTOTG,12)	=	Element/Gauss point event flags used for the major event file.
NI3	= LNODS(NELEM,NNODE)	=	Element connectivity matrix.
NI4	= LOCEL(NEVAB)	=	Global position of the element degrees of freedom (used in equation solution).
NI5	= MATNO(NELEM)	=	Element material property numbers.
NI6	= ISNEL(NELEM)	=	Element numbers to be output.
NI7	= ISNOD(NPOIN)	=	Node numbers to be output.
NI8	= NDEST(NEVAB)	=	Position in the front of the element degrees of freedom (used in equation solution).
NI9	= NDFRO(NELEM)	=	Element contribution to the frontwidth.
NI10	= NOFIX(NVFIX)	=	Nodal point number of constrained nodes.
NI11	= NOUTP(25)	=	Output print options.
NI12	= NPIVO(MBUFA)	=	Working buffer used in equation solution.
NI13	= NACVA(MFRON)	=	Active variable numbers in the front (used in equation solution).
NI14	= NAMEV(MBUFA)	=	Working buffer used in equation solution.
NI15	=	=	. . . . . Available

NIVAR = Length of blank common integer array for dynamic allocation of problem dependent integer arrays.

FILES USED BY THE FEM-CALC PROCESSOR

This appendix describes the contents and format of each file used by the FEM-CALC processor.

FORTRAN Logical Unit No. — Description

0 Console (n/a - KONS).
Used to display information concerning the progress and status of the calculations.

1 Force-Deflection File (FNAME4 - n/a).
File containing the force and displacement at each load step of a node specified by the user. The file is formatted and is suitable for importing into a separate program for plotting and postprocessing (i.e., Quattro Pro or Lotus 123).
Opened in START.

2 Element Major Event File (FNAME5 - n/a).
Print file containing a summary of the major events for the Gauss points of each element. The file is formatted and is suitable for printing.
Opened in MEVENT.

5 Standard FORTRAN Input (FNAME1 - IN).
File containing the problem input data as described in Section 5.2. The file is formatted in free form and is provided by the User.
Opened in SETUP.

6 Standard FORTRAN Output (FNAME2 - IO).
File containing an echo of all input data and the calculated results, including displacements, strains, stresses, and reactions. The file is formatted and has carriage control. It is suitable for printing.
Opened in SETUP and FCALC.

8 Load Increment File (FEM-08.LIF - n/a).
File containing the generated load increment data. The file is formatted.
Opened in START.

9 Equivalent Element/Nodal Point Load File (FEM-09.ELF - n/a).
File containing the equivalent nodal point loads due to
1) Concentrated nodal point loads.
2) Gravity loading.
3) Distributed edge loading.
These loads are stored by element based on the first appearance of a loaded nodal point. This file is used only if more than one of the three load types listed above are employed. The file is unformatted.
Opened in START.

FILES USED BY THE FEM-CALC PROCESSOR (Concluded)

FORTRAN Logical Unit No.	Description
11	Element Stiffness Matrix File (FEM-11.ESF - n/a). File containing the element stiffness matrices that are calculated and written in STIFRM. The file is used in FRONT to form the global stiffness matrix. The file is unformatted. Opened in START and RESTAR.
12	Reduced Frontal Equation File (FEM-12.FEF - n/a). File containing the reduced frontal equations, reduced load terms (right hand side), and bookkeeping information used in subroutine FRONT during the equation solution phase. This file is unformatted and is only used when the equation solution is out of core. Opened in START and RESTAR.
13	Restart File (FNAME6 - n/a). File containing the contents of memory resident variables and arrays, common blocks, and files necessary to restart the problem solution from the point the solution was terminated by a check point restart. The file is unformatted. Opened in RESTAR.
14	Reduced Loads File (FEM-14.RLF - n/a). File containing the reduced load terms (right hand side) used in subroutine FRONT during the equation solution phase. This file is unformatted and is only used when the equation solution is out of core. Opened in START and RESTAR.
15	Postprocessor Data File (FNAME3 - n/a). File containing a description of the mesh geometry and calculated results, including displacements, strains, stresses, and reactions. This file is unformatted and is used by the postprocessor to plot selected response quantities. Opened in START.
16	Initial Stress File (FEM-16.ISF - n/a). File containing initial stresses. This file is unformatted and is supplied by the user. Opened in START.

FEM-CALC MATERIAL PROPERTY ARRAY DESCRIPTION

The material properties are stored in a two-dimensional array PROPS(NMATS,NPROP). NMATS is the number of different materials and is set by the user at object time. NPROP is the number of properties available to define each material, and is preset by the computer program at 35. Some of the properties are defined by the user and some are calculated by the computer program from the user defined values. A description of the 35 properties are given in the following tabulation.

Variable	Description
PROPS(I,1)	Elastic modulus of the masonry in tension, E_t.
PROPS(I,2)	Poisson's ratio of the masonry, ν.
PROPS(I,3)	Element thickness, t (zero for axisymmetric problems).
PROPS(I,4)	Weight density per unit volume of the composite, ρ.
PROPS(I,5)	Tensile cracking strength of the masonry, f_{cr}.
PROPS(I,6)	Masonry strain at uniaxial compressive strength, ϵ_o.
PROPS(I,7)	Tension Stiffening (TS) Model No., MTS.
PROPS(I,8)	Exponential parameter α for TS Model No. 2.
PROPS(I,9)	Uniaxial compressive strength of masonry, f_m.
PROPS(I,10)	Compression Damage Parameter Model No., MCD.
PROPS(I,11)	Tension stiffening cutoff strain, start of cutoff.
PROPS(I,12)	Tension stiffening cutoff strain, end of cutoff.
PROPS(I,13)	Bilinear factor for the plastic modulus of the reinforcement, ζ.
PROPS(I,14)	Yield stress of the horizontal reinforcement, f_{yh}.
PROPS(I,15)	Elastic modulus of the reinforcement, E_s.
PROPS(I,16)	Yield stress of the vertical reinforcement, f_{yv}.
PROPS(I,17)	Strain hardening parameter, H'.
PROPS(I,18)	Vertical reinforcement ratio, ρ_v.
PROPS(I,19)	Horizontal reinforcement ratio, ρ_h.
PROPS(I,20)	Material model parameter, MMN. = 0, Elastic. = 1, Nonlinear reinforced masonry.
PROPS(I,21)	Tensile cracking strain of the masonry, ϵ_{cr}.
PROPS(I,22)	Yield strain of the horizontal reinforcement, ϵ_{hy}.
PROPS(I,23)	Yield strain of the vertical reinforcement, ϵ_{vy}.
PROPS(I,24)	Plastic modulus of the reinforcement, E_{sp}.
PROPS(I,25)	Initial elastic modulus of the masonry in compression, $E_m = A_1 f_m/\epsilon_o$.
PROPS(I,26)	Initial strain in vertical reinforcement (i.e., prestressing).
PROPS(I,27)	Initial strain in horizontal reinforcement (i.e., prestressing).
PROPS(I,28)	. . . . . (Reserved for future use).
PROPS(I,29)	Masonry compression unloading focal point factor, A_6.
PROPS(I,30)	Lower limit of the exponential branch for TS Model No. 2, B_1
PROPS(I,31)	Shape factor for the rising branch, A_1.
PROPS(I,32)	Shape factor for the initial falling branch, A_2.
PROPS(I,33)	Shape factor or lower limit for the exponential falling branch, A_3.
PROPS(I,34)	Shape factor for the attachment point of the exponential tail, A_4.
PROPS(I,35)	Strength enhancement factor, A_5.

FEM-CALC MAJOR EVENT FILE ARRAY DESCRIPTION

The major event file contains a record of the major events that have occurred during the calculation for each Gauss point of every element. The major events are stored in a two-dimensional array MEFIL(NTOTG,12). The number of rows, NTOTG, corresponds to the total number of Gauss points in the mesh (i.e., NGAUS•NGAUS•NELEM). Columns 1 through 8 and 11 through 12 of MEFIL correspond to different major events as described in the following tabulation. Columns 9 and 10 of MEFIL contains an encoded set of flags that are used to update the data in the other columns. The tabulation also gives the encoding in the square brackets.

Variable	Description
MEFIL(I,1)	Load increment at which first tensile cracking occurs in the masonry ($\epsilon_t > \epsilon_{cr}$). [Programming Encode Key, M = M + 1]
MEFIL(I,2)	Load increment at which the masonry peak strength is reached ($\epsilon_c < \epsilon_p$). [Programming Encode Key, M = M + 2]
MEFIL(I,3)	Load increment at which masonry crushing occurs ($\epsilon_c < \epsilon_e$). (Not used) [Programming Encode Key, M = M + 10]
MEFIL(I,4)	Load increment at which yielding of the vertical reinforcement occurs ($\epsilon_y > \epsilon_{yv}$). [Programming Encode Key, M = M + 20]
MEFIL(I,5)	Load increment at which yielding of the horizontal reinforcement occurs ($\epsilon_x > \epsilon_{yh}$). [Programming Encode Key, M = M + 100]
MEFIL(I,6)	Load increment at which the damage factor, β, is invoked. [Programming Encode Key, M = M + 200]
MEFIL(I,7)	Maximum value of the tensile crack orientation in the masonry (updated when MEFIL(I,1) is positive).
MEFIL(I,8)	Minimum value of the tensile crack orientation in the masonry (updated when MEFIL(I,1) is positive).
MEFIL(I,9)	Encoded flag used to update data after convergence has been reached for principal direction 1.
MEFIL(I,10)	Encoded flag used to update data after convergence has been reached for principal direction 2.
MEFIL(I,11)	Maximum value of the tensile (+) or compressive strain (-) in the vertical reinforcement in milli-strain (i.e., strain x 10^3).
MEFIL(I,12)	Maximum value of the tensile (+) or compressive (-) strain in the horizontal reinforcement in milli-strain (i.e., strain x 10^3).

APPENDIX C

DEFINITION OF INPUT DATA FOR EARLIER VERSIONS

The differences for Versions 100 to 104 are:

- Problem Control Parameters, Card Group 3.
- Material Property Data, Card Group 7.
- Load Increment Controls, Card Group 18.

The definition of the required input data for these card groups of Versions 100 to 104 is given on the following pages.

Card Group 3	Problem Control Parameters	Versions 100 to 104
No. of Records	1	
Format	Free Field	

Variable	Description	Notes
NPOIN	Total number of nodal points.	
NELEM	Total number of elements.	
NVFIX	Total number of constrained nodal points, where one or more degrees of freedom are restrained or have prescribed displacements.	
NTYPE	Problem type parameter. = 1, Plane stress = 2, Plane strain = 3, Axisymmetric	
NNODE	Number of nodes per element. = 4, Linear quadrilateral element = 8, Quadratic quadrilateral element = 9, Quadratic quadrilateral element	
NMATS	Total number of different materials.	
NINCS	Number of increments in which the total loading is to be applied.	
IPFLAG	Postprocessor parameter. = 0, A postprocessor file is not generated. = 1, A postprocessor file is generated as specified in Card Group 18.	
INISR	Initial stress parameter. = 0, No initial stress = 1, Initial stresses generated from linear distribution given in Card Group 8. = 2, Initial stresses read from a file. = 3, Initial stresses to be written to an initial stress file.	
IREST	Restart parameter. = 0, A restart file is not generated at the end of the run. = 1, A restart file is generated at the end of the run. Go to Card Group 4.	

Card Group 7	Material Property Data	Versions 100 to 104
No. of Records	NMATS Sets	
Format	Free Field	

Variable	Description	Notes
	Record 1 Material ID	
NUMAT	Material identification number.	
	Record 2 - n Material Properties	(1)
PROPS(1)	Elastic modulus of the masonry, E_t, in tension.	
PROPS(2)	Poisson's ratio of the masonry, ν.	
PROPS(3)	Element thickness, t. Zero for axisymmetric problems.	
PROPS(4)	Weight density per unit volume of the composite.	
PROPS(5)	Tensile cracking strength of masonry, f_{cr}.	
PROPS(6)	Masonry strain at uniaxial compressive strength, ϵ_o.	
PROPS(7)	Tension Stiffening (TS) Model No.	
PROPS(8)	Parameter α for TS Model No. 2.	
PROPS(9)	Uniaxial compressive strength of masonry, f_m.	
PROPS(10)	Compression Damage Parameter Model No. = 1, Use β from Equations (3-14, 3-15, & 3-16). = 2, β = 1.0.	
PROPS(11)	Reserved for future use.	
PROPS(12)	Reserved for future use.	
PROPS(13)	Reserved for future use.	
	Continued	

Card Group 7	Material Property Data (Concluded)	Versions 100 to 104
No. of Records	NMATS Sets	
Format	Free Field	

Variable	Description	Notes
	Record 2 - n Material Properties (Concluded)	(1)
PROPS(14)	Yield stress of the horizontal reinforcement, f_{yh}.	
PROPS(15)	Elastic modulus of the reinforcement, E_s.	
PROPS(16)	Yield stress of the vertical reinforcement, f_{yv}.	
PROPS(17)	Strain hardening parameter, H'.	
PROPS(18)	Vertical reinforcement ratio, ρ_v.	
PROPS(19)	Horizontal reinforcement ratio, ρ_h.	
PROPS(20)	Material Model Parameter. = 0, Elastic. = 1, Nonlinear reinforced masonry.	
	Go to Card Group 8.	
NOTES:		
(1)	All 20 material properties must be supplied; and since the values are input in free field format, the number of records will depend on how the user enters the data.	

Card Group 18	Load Increment Controls	
No. of Records	Variable (1)	
Format	Free Field	
Variable	**Description**	**Notes**
NDIV	Number of divisions used to generate load increments between the preceding input record in this card group and this input record.	(1,2)
FACTL	Total loading factor for applied force loading defined in Card Groups 13 to 17.	(5)
FACTD	Total loading factor for the prescribed displacements defined in Card Group 6.	(5)
TOLER	Convergence tolerance factor, defined in percent (i.e., 5% = 5.0).	(3)
MITER	Maximum number of iterations to be used for the generated load increment.	(3)
NOUTP	Parameter controlling output of the results for the final iteration of the generated load increment. = 0, No output. = 1, Output displacements. = 2, Output displacements and reactions. = 3, Output displacements, reactions, and element stresses and strains.	(4)
NALGO	Solution algorithm control parameter. Stiffness Matrix is Updated at: = 1, 1st Iteration of 1st Load Increment = 2, 1st Iteration of Each Load Increment = 3, 1st Iteration of This Load Increment	(3)
NPLOT	Postprocessor file flag. = 0, Do not generate a postprocessor record for this load increment. = 1, Generate a postprocessor record for this load increment. Continued	(4)

Card Group 18	Load Increment Controls (Concluded)	
No. of Records	Variable (1)	
Format	Free Field	
Variable	**Description**	**Notes**
NREST	Restart flag. = 0, Do not generate a restart file at the end of this load increment. = 1, Generate a restart file at the end of this load increment and terminate execution. End of input.	(4)
NOTES:		
(1)	This card group is terminated when NDIV is set to a negative number. All data on the last card is ignored.	
(2)	Load increments (displacements and forces) are generated between successive load increment input records given in this card group.	
(3)	Invoked for all generated load increments.	
(4)	Invoked only on the last load increment.	
(5)	The applied force loading and prescribed displacements are applied incrementally at sequential load steps, and the incremental amount applied at each load step is calculated from the parameters NDIV, FACTL, and FACTD. The factors FACTL and FACTD are input as total quantities that define the level to be reached at the end of the generated load increments.	